Review article

Magnetic particle targeting for diagnosis and therapy of lung cancers

Mahsa Saadat[a,1], Mohammad K.D. Manshadi[b,a,1], Mehdi Mohammadi[a,b,c,d,1],
Mohammad Javad Zare[e], Mohammad Zarei[f], Reza Kamali[g], Amir Sanati-Nezhad[b,c,*]

[a] Department of Chemical Engineering, College of Engineering, Shahid Bahonar University of Kerman, Kerman, Iran
[b] Department of Mechanical and Manufacturing Engineering, University of Calgary, Calgary, Alberta T2N 1N4, Canada
[c] Center for Bioengineering Research and Education, University of Calgary, Calgary, Alberta T2N 1N4, Canada
[d] Department of Biological Science, University of Calgary, Alberta T2N 1N4, Canada
[e] Medical College, Islamic Azad University, Tehran, Iran
[f] Mitochondrial and Epigenomic Medicine, and Department of Pathology and Laboratory Medicine, Children's Hospital of Philadelphia and Perelman School of Medicine,
University of Pennsylvania, Philadelphia, PA 19104, USA
[g] Department of Mechanical Engineering, Shiraz University, 71345 Shiraz, Iran

ARTICLE INFO

ABSTRACT

Over the past decade, the growing interest in targeted lung cancer therapy has guided researchers toward the cutting edge of controlled drug delivery, particularly magnetic particle targeting. Targeting of tissues by magnetic particles has tackled several limitations of traditional drug delivery methods for both cancer detection (e.g., using magnetic resonance imaging) and therapy. Delivery of magnetic particles offers the key advantage of high efficiency in the local deposition of drugs in the target tissue with the least harmful effect on other healthy tissues. This review first overviews clinical aspects of lung morphology and pathogenesis as well as clinical features of lung cancer. It is followed by reviewing the advances in using magnetic particles for diagnosis and therapy of lung cancers: (i) a combination of magnetic particle targeting with MRI imaging for diagnosis and screening of lung cancers, (ii) magnetic drug targeting (MDT) through either intravenous injection and pulmonary delivery for lung cancer therapy, and (iii) computational simulations that models new and effective approaches for magnetic particle drug delivery to the lung, all supporting improved lung cancer treatment. The review further discusses future opportunities to improve the clinical performance of MDT for diagnosis and treatment of lung cancer and highlights clinical therapy application of the MDT as a new horizon to cure with minimal side effects a wide variety of lung diseases and possibly other acute respiratory syndromes (COVID-19, MERS, and SARS).

1. Introduction

The respiratory tract is the most vulnerable part of the body affected by various diseases, such as idiopathic pulmonary fibrosis, chronic obstructive pulmonary disease (COPD), asthma, and cancer [1]. Among these diseases, lung cancers are 11.6% of the total diagnosed cancers worldwide, with 18.4% mortality [2]. In the United States, lung and bronchus cancers accounted for above 147,000 death in both sexes in 2019 [3].

Lung tumors have been classified based on different stages of progression, including small cell lung carcinoma (SCLC) and non-small cell lung carcinoma (NSCLC) (Fig. 1) [4–6]. Small-cell carcinoma (SCLC) accounts for almost 15% of lung cancers, primarily caused by tobacco

smoking, and mainly occurs by narrowing of bronchial airways [4]. The SCLC is classified as limited-stage (LS) and extensive stage (ES) depending upon the presence or absence of metastases [7]. In LS-SCLC, tumors are inside the lung or nearby lymph nodes, while in ES-SCLC, tumors spread to distant organs like chest [8]. Various treatments have been developed to selectively target each stage of SCLC cancers. The most known treatment of LS-SCLS is a combination of chemotherapy with chest radiotherapy (RT) given its high responsiveness, which may, with high probability, stop cancer retrieving, cure or shrink the tumor, and suppress the symptoms of cancer [9].

On the other hand, NSCLC is widely encompassed, accounting for almost 85% of all lung cancers. The most common type of NSCLC is adenocarcinomas that spread to lymph nodes and multiple sites in the
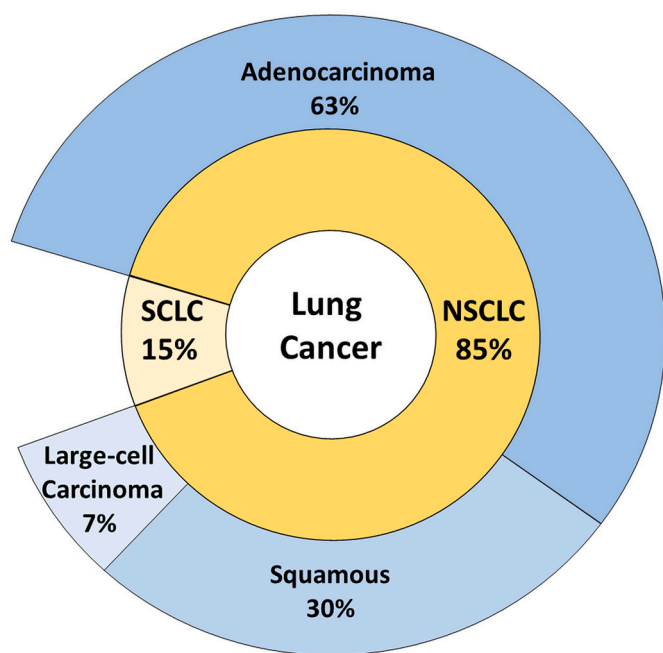
Fig. 1. Lung cancer classifications [4].

lungs like alveolar walls [10]. Squamous cell carcinomas, on the other hand, arise in the central chest area of bronchi and grow large and forming a cavity [11]. The least common type of this category is large cell carcinomas, spreading to the lymph nodes and distant sites [12]. However, several subtypes of NSCLC are much less common, e.g., adenoid cystic carcinomas, lymphomas, and sarcomas. These subtypes originate from salivary glands, white blood cells (lymphocytes), and mesenchymal (connective) tissue, spreading to the lungs through the bloodstream or lymphatic system [13].

Three factors of tumor size (T), spreading of a tumor to adjacent nodes (N), and metastasis to nearby tissues (M) determine the progression of lung cancers [14]. Imaging methods such as magnetic field X-rays [15,16], sound waves [17], and radioactive substances [18] are known to be used before and after the diagnosis of lung cancer to determine where cancer cells spread and what would be the most efficient treatment approach. Among various imaging techniques, magnetic resonance imaging (MRI) generates the most detailed structural images of the tumor [19,20]. Upon determining the stage of the tumor, the extent of cancer, and the overall health and function of the lungs, a proper therapeutic procedure needs to be selected. Different stages of the NSCLC and corresponding types of treatments are summarized in Table 1 [14,21–23]. The surgery is the primary treatment advice for stage 0 lung cancer to remove the tumor. The higher the number of cancer cells, the more chance of spreading cancer, necessitates combining chemotherapy and radiation besides the surgery [24].

Chemotherapy is normally used to vanish tumor cells, although it may also contribute to side effects on healthy cells or even elevating the tumor growth [26]. It may also has a negative impact on the body via one or a combination of alopecia, fatigue, neutropenia, nausea and vomiting, sore mouth, gastrointestinal and renal toxicity [27–30]. In this regard, targeted delivery of drugs has been considered as a promising method to reduce the harmful effect on healthy tissues [31]. Moreover, the carriers of drugs can produce image contrast and therefore provide brighter images from the tissues needed for screening purposes [32].

Nanoparticles, as the carriers of drug administration, have provided an excellent opportunity to practice optimal targeting strategies in the lung for both diagnosis and treatment purposes. Several review articles have overviewed the efficacy of nanoparticle carriers for cancer

therapy. For example, the performance of pH-sensitive nanoparticle carriers in targeted cancer therapy was reviewed by Kanamala et al. [33]. Nano-liposomes loaded with ligands or antibodies have been reviewed for their performance in the therapy of lung cancers. Najeeb Ullah et al. [34] provided in-depth insight into the site-directed application of nano-liposomes to release their encapsulated drugs to tumor areas. On the other hand, the appropriate design of the drug-carrier complex is key for successful drug delivery. Rizvi and Saleh [35] in 2018 reviewed the design and application of nanoparticles-drugs to target tumors with the least side toxicity and less frequent dosing. Sun et al. [36] overviewed the utility of magnetic nanoparticles in MR imaging for cancer diagnosis. They proposed new strategies to improve the imaging contrast by incorporating surface coatings (gold, silica, and biocompatible polymers) or employing higher strength magnetic core (e.g. doped iron oxide nanocrystals, nanocomposites and metallic/alloy nanoparticles).

Targeted cancer treatment using nanomedicine has been performed by the release of particles in the blood circulation or respiratory system [37,38]. The main dispute though, is to entrap particles in the desired location. The targeted delivery methods are divided into two main groups: passive methods without using any external forces, and active methods that utilize an external energy source to navigate nanoparticles to the location of interest. In the passive targeting, drugs are usually coated with substances like polyethylene glycol (PEG) [39], polyglutamic acid (PGA) [40], polylactic-co-glycolic (PLGA) [41], and polysaccharides such as cyclodextrin [20] to bind with oxygen to extend the time of stay in the bloodstream and boosting the efficiency of treating the diseased tissue [42]. In active methods, an external force such as a magnetic field [43] or ultrasound is employed [44] to steer drugs toward the desired tissue. Alternatively, a responsive material [45] or a cell-specific ligand [46] is exploited to improve the affinity of drugs to target cells. Among various active methods, MDT has demonstrated to be a promising approach for high efficacy drug delivery due to its fewer side-effects, quick response, and low cost [47,48]. The MDT methods have been extensively investigated by researchers through different *in vivo*, *in vitro*, and numerical simulation studies [43,49–51]. Also, it has been used for lung cancer diagnosis and therapy [52], inhalable drug delivery [53,54], intracellular drug delivery [55]. In this method, drug is loaded on magnetizable porous micro/nano particles. These drug-conjugated particles can be manipulated throughout their journey in the body by a magnetic field, captured in the target location, and released in the desired tissue to perform treatment on the organs such as lung [56,57]

It is noted that the real-time and sensitive measurement of the distribution of nanoparticles in small animals is challenging and very expensive [36,58,59]. Computational fluid dynamic (CFD) methods have instead supported the prediction of MNPs fates in various human tissues [60–64]. Numerical simulations have also enabled to investigate complex drug delivery scenarios that are difficult to implement *in-vivo* and *in-vitro*, therefore they offer valuable insights for the transport and deposition of drugs into target tissues [64,65].

This review discusses clinical features of the lungs, experimental techniques and numerical methods developed for MDT studies, and advances in new technologies utilized to implement MDT in the lungs with the focus on lung cancer diagnosis and treatment. It further highlights the challenges and future perspectives of developing efficient MDT strategies based on the clinical features of the lungs.

2. Pathology of lung cancers and clinical features

Lung carcinoma accounts for a vast majority of primary lung tumors, while a smaller portion is related to other categories such as carcinoids, mesenchymal malignancies, lymphomas, and a small number of benign lesions. Patients within 50-70 years old constitute the largest group of lung carcinoma patients [66]. More than half of these patients already have distant metastases when detected with lung

Table 1

Stages of non-small cell lung carcinoma (NSCLC) and corresponding treatment methods

No. of stage	Definition of NSCLC's stage	Treatments of NSCLC
Hidden cancer	The tumor size is too small to be distinguished by imaging tests and bronchoscopy. There is no node (N0) and no metastasis (M0); therefore there is no tumor found in the lung while there exist cancer cells in sputum.	Surgery
Stage 0	The tumor known as carcinoma in situ is found at the lining layer of the lung airways. Cancer cells have not yet spread into the lungs tissue (M0, N0)	Surgery- stereotactic body radiation therapy (SBRT)- radiofrequency ablation (RFA)
Stage I	This stage is divided into two subdivisions: The tumor invaded across the lung tissue but in less than ½ cm, N0 (no nodes)- M0 (no metastasis)	Surgery to remove part of the lung (a lobectomy) or all the lung (pneumonectomy)
	The tumor is about 1 cm, N0 (no nodes) - M0 (no metastasis). It is invaded across the lung membrane without any effect on the bronchi or branches.	Radiotherapy and radiofrequency ablation are alternative treatments for patients with serious physical problems.
Stage II	The tumor is larger than 3 cm- M0 (no metastasis)- it spreads through the carina (causes clogging the airway) or into the chest wall	Surgery and chemotherapy are recommended to reduce the chance of cancer return.
Stage III	The tumor is larger than 5 cm in size and spreads into blood vessels, trachea and esophagus- M0	Surgery to remove all the tumor, then chemotherapy, along with radiotherapy.
Stage IV	Any size of tumor spreading to nearby nodes as well as other organs like bones, brains and liver. The survival rate of stage IV is 1%, owing to the extent of tumor growth and invasion [25].	Based on the tumor location, individual or combination of the following methods are utilized - Surgery - Chemotherapy - Targeted therapy - Radiotherapy -Immunotherapy - Photodynamic therapy (PDT)

carcinoma, and about 25% of them have the illness in the regional lymph nodes [67].

2.1. Morphology of lung carcinoma

Compared to other types of lung cancer, adenocarcinomas grow at a slow pace and generates smaller masses. However, it is able to metastasize extensively in the initial stages of the disease [68]. Currently, adenocarcinoma is the most widespread type of lung cancer, being accounted for about 50% of lung cancers diagnosed [66]. Typical adenomatous hyperplasia (AAH) is supposed to presage adenocarcinoma [69], which follows a stepwise process to adenocarcinoma in situ, minimally invasive adenocarcinoma (with a diameter smaller than 3 cm and an invasive component of smaller than 5 mm), and invasive adenocarcinoma (various-sized tumors with an area of invasion larger than 5 mm). Adenocarcinoma in situ (AIS) usually includes peripheral portions of the lungs as the nodules [70,71].

A majority of squamous cell carcinomas (between 60% to 80%) emerge in the proximal parts of the tracheobronchial tree following a series of squamous metaplasia-dysplasia-carcinoma in situ. However, it is growingly emerging as peripheral lesions [72,73]. Central necrosis with consequent cavitation might be displayed by central and peripheral squamous cell carcinomas [74,75]. A small group of central, well-differentiated squamous cell carcinomas appears as exophytic, endobronchial, papillary lesions. Patients who experience this unique form of squamous cell carcinoma often show permanent cough, repeated hemoptysis, or relapsing pulmonary infections resulting from airway blockage. A majority of patients with exophytic endobronchial squamous cell carcinoma have been detected with low-grade disease and a suitable prognosis, which could lead to a greater than 60% five-year survival rate [76]. Finally, the small neoplasm comes to asymptomatic phase, when a distinguished tumor mass starts blocking the lumen of the main bronchus, usually leading to distal atelectasis and infection [75]. Undifferentiated malignant epithelial tumors in which no glandular or squamous differentiation could be observed are categorized as large cell carcinomas. LCC is often a sizeable peripheral mass with notable necrosis [68].

The SCLCs usually emerge as pale gray masses, position centrally, and expand into the lung parenchyma [77,78]. Most of these tumors have already metastasized to hilar and mediastinal lymph nodes when they are detectable. SCLCs generally tend to grow faster, more central and mediastinal localization and have quicker metastasis to extrathoracic sites with shorter total survival periods [79,80]. Normally, a simplified system of clinical finite or clinical broad disease manages small cell carcinoma. The main duty of tumor/node/metastasis (TNM) staging in SCLC is to enhance the specificity of information included in clinical cancer registries and clinical research. In the 18th edition of the TNM system, some analyses were conducted which verify the relevance of the TNM system to small cell lung cancer and its prognostication capability, while for more advanced stages, the survival rate is aggravated [81].

2.2. Clinical features of lung cancer and metastasis

All types of lung cancers tend to extend to lymph nodes in the carina, the mediastinum, the neck (scalene nodes), clavicular areas, and finally, to distant locations. The participation of the left supraclavicular node (Virchow node) is the specific common feature and, on occasions, draws awareness to a primary occult tumor. Lung carcinoma is insidious lesions that often have extended to an unrespectable state before any symptom emerges [68,79].

Bone, brain, spine, and nerve are among the organs often involved in metastatic NSCLC [82,83]. Adrenal gland nodules or masses exist in possibly 3-4% of patients during the early diagnosis, which is mainly benign in patients with NSCLC [84,85]. Metastases rarely occur in the liver solely (3%). A majority of liver lesions in NSCLC patients are benign cysts or hemangiomas [86]. The direct spread of the primary tumor to the pleura or chest wall [87] is common. Also, pleural diseases are commonly displayed clinically as metastases associated with pleural effusion [88,89]. Bone and respiratory system metastases are more common in adenocarcinoma. Small cell lung cancer commonly leads to liver and nervous system metastases. Also, metastasis to the nervous system occurs more often in women (43% with respect to 35% for men) and younger patients [67].

According to Riihimäki et al. [67], sex, histological subtype, and age affect the metastatic sites and survival in metastatic lung cancers. Liver and bone metastases indicate low survival in comparison with nervous system metastases. They also reported that the most recurring metastatic locations were the nervous system, bone, liver, respiratory system, and adrenal gland. Non-metastatic and metastatic lung cancers correspond to median survival after diagnosis equal to 13 months and 5 months, respectively. It was also revealed that liver metastases presented the worst prognosis (3 months), particularly for large cell histology. Poor survival is also observed for bone metastases, while a

better survival is reported for respiratory and nervous system metastases [67].

Overall, squamous cell carcinoma and adenocarcinoma present a more favorable prognosis than SCLC, and if they are diagnosed prior to metastasis or local spread, they may be cured by lobectomy or pneumonectomy [68,90]. Specific inhibitors could have significant effects on unresectable adenocarcinomas related to targetable mutations in tyrosine kinases such as Epidermal Growth Factor Receptor (EGFR) [91]. On the other hand, SCLCs are already extended when they are diagnosed, even if the primary tumor seems to be tiny and localized, therefore, surgical resection could not be considered as a feasible solution. Even with therapy, the median survival does not exceed one year, and only 5% of patients survive for 10 years [92,93].

2.3. Pathogenesis of lung cancers

The genetic instability in human cancers appears to exist at two levels: at the chromosomal level, that includes large scale losses and gains, and at the nucleotide level, including single or several base changes [94]. Like other cancers, lung carcinomas arise by the accumulation of driver mutations resulting in the transformation of benign progenitor cells in the lung into neoplastic cells presenting many cancer hallmarks [68,95]. Lung cancers harbor many numeric chromosome abnormalities and structural cytogenetic abnormalities, including deletions and nonreciprocal translocations. At least three classes of cellular genes are involved: proto-oncogenes, tumor suppressor genes (TSGs), and DNA repair genes. Oncogenic activation often occurs via point mutation, gene amplification, or gene rearrangement. TSGs are classically inactivated by the loss of one parental allele combined with a point or small mutation or methylation inactivation of a target TSG in the remaining allele. Current published studies have not yet confirmed a prominent role for abnormalities of DNA repair genes in lung cancers, including DNA mismatch repair genes, although an alteration in simple repeat sequences has been observed [96]. The primary molecular alterations in lung cancers are summarized in Table 2.

3. Magnetic particle targeting for diagnosis and screening of lung cancers

Nanoparticles have been used in various imaging methods such as computed tomography (CT) [116], magnetic resonance imaging (MRI) [117], and near-infrared (NIR) imaging [118] for detection of lung cancers. Chest X-rays and low dose CT-scans provide pictures to show size, shape, and position of cancer cells in lymph nodes [15]. CT-scan has disadvantages like causing severe artifacts in images by internal organ motion and tattoos along with low sensitivity (55–65%) and low specificity (65–75%) [119,120]. The CT-scan and X-rays are unable to provide detailed images of soft tissues like inside the lungs, cartilages, joints, or muscles. More importantly, the amount of radiation exposed to patients due to CT or X-rays imaging may increase the risk of cancer, along with the occurrence of false-negative results when no lung cancer is found consequently [121,122]. Positron emission tomography (PET) has challenges with differentiating metastatic or non-metastatic nodes [120,123]. While the combination of CT-scan and PET showed a better outcome in lung cancer imaging, but they still have restrictions in detecting non-resectable lung cancers [124]. On the other hand, the MRI has been utilized extensively for lung cancer diagnosis due to its decent non-invasiveness and effectiveness. Also, utilizing magnetic MNPs in MRI provides a high contrast for generating the most detailed imaging. For instance, magnetic iron oxide (Fe_3O_4) nanoparticles have been used for MR imaging of the lungs because of their excellent biocompatibility and magnetization as well as their proper drug uptake and release [125–127]. Water-dispersible PEI-coated Fe_3O_4 NPs have been used for MRI-based tumor imaging [126]. More importantly, tracking of drug-loaded superparamagnetic iron oxide nanoparticles (SPIONs) in the lungs has shown to be feasible for imaging via an external magnetic

field. The endothelial progenitor cells (EPCs) stabilized with super-magnetic iron oxide (SPIO) were used for cancer ablation and repair of vascular injury, meantime they facilitate MRI imaging of lung cancers by providing the patterns of EPCsin tumor cells [128]. Also, the non-toxic and stable drugs folate-conjugated polyethylene glycol (FA-PEG) SPIONs were prepared as an efficient imaging agent for active targeting in the in-vivo models of lung cancers [129]. Cell-mediated delivery of nanogels loaded with Fe_3O_4 is another effective and novel targeted nanoplatform for increasing the MR contrast of images from lung tumors [130]. In addition, Dextran-Benzoporphyrin Derivative (BPD) loaded in SPIONs is another novel nanomedicine drug for treating lung cancers while applicable for lung cancer imaging, where they enhance the MRI contrast [131]. Guthi et al. [132] encapsulated superparamagnetic iron oxide (SPIO) with doxorubicin in micelle cores as the MRI contrast agent. Moreover, the size and surface chemistry of MNPs are elemental characteristics of these particles, determining their route of delivery [133]. Different nano-carries such as liposomes, dendrimers, polymeric micelles, and inorganic magnetic particles have been used for active targeting in lung cancer imaging [53]. For instance, the optimal size of NPs is known to be 10-100 nm to ensure that they are not sequestered by the spleen or removed through the kidney [134]. MNPs with improper size may also accumulate in the spleen, brain, and liver, therefore the overall size of MNPs with their coating should not exceed 100 nm [135]. The utilization of MNP contrast agents in MRI imaging of the lungs has enabled the detection of solid pulmonary nodules (SPNs), characterization of SPNs, staging of lung cancers, and prediction of tumor treatment response [136].

MR imaging has also been combined with other imaging techniques to improve the diagnosis of lung cancers. Chang et al. [137] used new iron oxide NPs with dual optical and magnetic properties to enable combined MRI and diffusion-weighted imaging (DWI) in order to monitor the early response of lung cancers to chemoradiation. Such combinatory imaging technique has not been clinically practiced due to the low apparent diffusion coefficient of MNPs [138]. Yoon et al. [139] further used combined PET/MRI with appropriate MNP contrast agents for lung cancer detection. The work was successful to identify tumor necrosis, hypoxia, and heterogeneity of the tumor microenvironment. Although the ultrasonic nebulization system was employed for respiratory drug delivery [140], the first SPIO nano-platform was utilized for lung cancer imaging *in-vivo* to enhance imaging sensitivity with the magnetic resonance-guided focused ultrasound surgery (MRgFUS) [44]. MRgFUS is a thermal treatment method used for various types of cancers in soft tissues like prostate, kidney, and liver [44]. The key challenge of MRgFUS for *in vivo* applications is related to its high ultrasound power, which may result in skin burns, edema, perforation of intestines, and injury of peripheral nerve surrounding the tumor. This challenge has been addressed by the SPIO nanoplatform with a demonstrated MRI effectiveness and tumor-ablative efficacy for lung cancer treatment [44]. Also, the potential of a combined MDT MRgFUS and MDT methods was further demonstrated for brain cancer treatment [141]. Moeier-Schroers et al. [142] compared MRI and low-dose CT (LDCT) for lung cancer detection, where they showed that the MRI has excellent sensitivity and specificity for the primary screening of lung cancer patients with the capability in prediction of nodules. The effectiveness of different MRI methods and their combination with other imaging techniques utilized for lung cancer detection are presented in Table 3.

4. Intravenous magnetic drug targeting (MDT) for lung cancers

The magnetic field has been extensively used as an external source to steer drug particles into the circulatory system and targeted tissues, such as heart [173], lung [174], and brain diseases [175]. Magnetic nanoparticles are circulated throughout the blood vessels, and their encapsulated drugs are trapped in the region of interest under the magnetic field exerted from a stent, core, or a permanent magnet [127,176]. The advances in MDT modeling of intravenous drug delivery

Table 2

Primary molecular alterations detected in lung cancers

Abnormality	Description	Small cell lung carcinoma	Non-small cell lung carcinoma
EGFR mutation	Epidermal Growth Factor Receptor (EGFR) is a receptor tyrosine kinase which stimulates downstream pro-growth pathways and signaling molecules [97]	NA	About 15-30% of non-Asian patients and 30-60% of Asian patients with adenocarcinoma harbor a mutation of the *EGFR* gene [97]; Observed in approximately 15% of NSCLC adenocarcinomas in the United States [97,98].
RAS mutations	Mutations in *KRAS* promotes growth and prevents apoptosis	Rare [68,99]	Observed in approximately 20-25% of lung adenocarcinomas in the United States; Generally associated with smoking [100]
ALK rearrangements	This rearrangement involves the anaplastic lymphoma kinase (*ALK*) tyrosine kinase	NA	Present in approximately 4% of NSCLC adenocarcinomas [101]; Observed in 2-7% of United States patients with NSCLC [97]
ROS1 rearrangements	c-ROS oncogene 1 (ROS1) is a receptor tyrosine kinase which acts as a driver oncogene	NA	Present in 1-2% of NSCLC with a genetic translocation between *ROS1* and other genes, especially *CD74* [102,103]
BRAF mutation	*BRAF* is a downstream signaling mediator of Kirsten rat sarcoma viral oncogene homolog (*KRAS*), a gene that acts as an on/off switch in cell signaling; KRAS activates the mitogen-activated protein kinase (MAPK) pathway which is involved in sending signals inside cells, involved in directing cell growth [104,105].	NA	Present in 1-3% of NSCLCs; Usually associated with a history of smoking [104,105]
NTRK fusion	Fusions involving one of three tropomyosin receptor kinases (*TRK*); The TRK family contains three members, TRKA, TRKB, and TRKC [106].	NA	Present approximately in 1% of NSCLC [106].
HER2 mutation	HER2 (*ERBB2*) is an EGFR family receptor tyrosine kinase [107,108].	NA	Present approximately in 1 to 3 percent of NSCLC tumors [107,108]
MET abnormalities	MET is a tyrosine kinase receptor for a hepatocyte growth factor (HGF).	c-MET mutation present [109]	MET abnormalities (drug *MET* exon 14 skipping mutations) are present in 3% of lung adenocarcinomas; *MET* and *EGFR* co-mutations are present in 5 to 20 percent of *EGFR*-mutated tumors which are resistance to EGFR inhibitors [110–112].
3p depletions	Inactivation of the putative tumor suppressor genes [113] located on the short arm of chromosome 3 (3p) is a very common early event [68].	A very common tumor suppressor gene abnormality in SCLCs [99]; Present in more than 90% of SCLCs [68]	Present in more than 80% of NSCLCs [68]
RB mutations	The retinoblastoma gene is mutated in several types of human cancers [114].	A very common tumor suppressor gene abnormality in SCLCs [99]; Present in about 90% of SCLCs [68]	Present in about 20% of NSCLCs [68]
TP3 mutations	TP53 is a tumor suppressor gene which is most commonly affected by point mutations in cancers; occurs relatively late [115].	A very common tumor suppressor gene abnormality in SCLCs [99]; Present in more than 90% of SCLCs [68]	Present in more than 50% of SCLCs [68]

to the lungs are discussed below and classified in Table 5.

4.1. In vivo MDT models for intravenous drug delivery to the lungs

The MNPs are injected throughout the blood and steered to the desired tissues under the influence of the magnetic field. The low dose of anticancer drugs can be employed in the presence of a magnetic field to avoid the aggregation of magnetic nanoparticles in the blood [177]. Various MDT methods have been used to employ smaller dosages of drugs and to reduce the toxicity of chemotherapeutic agents in the untargeted tissues [178]. Mykhaylyk et al. [179] conducted

Doxorubicin magnetic conjugate (DOX-M) nanoparticles in the presence of a 0.2 T magnetic field in mice model. The effect of magnetic field on DOX-M was evaluated in the lungs by employing a non-uniform magnetic field over the left lung. The results showed that the increase in the intensity of the magnetic field causes a considerable accumulation of DOX-M in the lung, therefore this method is a promising method for DOX-M pharmacokinetics. Wu et al. [180] further utilized dextran-modified nanoparticles and an external magnetic field for healthy rats to evaluate the accumulation of nanoparticles coated with Fe_3O_4 in the lung, liver, and spleen. The magnetic field helped to control biodistribution pattern of nanoparticles in the liver and spleen than in the

Table 3

Single or combinatory MR imaging for cancer treatment

Imaging methods	Sensitivity/ specificity	Advantages	Disadvantages	Refs.
MRI	Sensitivity: 80.5%-100% Specificity: 73%-87%	- Rapid - No radiation exposure - Less cost - Easy accessibility - Differentiating metastatic from non-metastasic nodes	- Negative effect on images quality caused by a motion of artifacts (breathing, cardiac movement, patient movement)	[136], [124,143], [144], [145], [146]
MRI/PET	Sensitivity: 96%-100% Specificity: 61%	- Excellent image quality - No artifacts in images - High accuracy	- Long examination time - Difficult access	[147], [148], [149]
MRI/DWI	Sensitivity: 87% Specificity: 88%	Beneficial for diagnosis of malignancy and benignity in the lungs	- 30 min test time	[150], [124], [138]

lungs. Elbialy et al. [181] further used magnetic gold nanoparticles (MGNPs) loaded with doxorubicin (DOX) to investigate their distribution in the liver, lungs, and spleen. They employed permanent magnet (magnetic field strength was 1.14 T) in female Balb/c mice at different conditions of injection to investigate the possible deep penetration of DOX into target tissues. The results demonstrated the successful targeted delivery of MGNPs-DOX to the tumors compared to either free DOX (without MGNPs) or the absence of the permanent magnet. Vlaskou et al. [182] injected nucleic acid carriers under the influence of the combined magnetic field and ultrasound. The results showed a higher accumulation of drugs in the lungs of mice for the combinatory stimulation system than every one of the magnetic or ultrasound systems. To further enhance the efficacy of drug delivery, Jia et al. [183] introduced DOX-loaded MNPs and MNPs directly into solid tumors and monitored the effect of drugs in the presence and absence of an external magnetic field. The results showed that the tumor size decreased significantly for Dox-MNPs in the presence of an external magnetic field (0.5 T) rather than free DOX or the Dox-MNPs in the absence of magnetic field. The rate of metastasis was reported to be 50%, 60% and 87% for DOX-loaded MNPs under the magnetic field, DOX-loaded MNPs with no magnet, and control (drug-free), respectively [183]. It is noted that the maximum threshold of the applied magnetic field should not exceed 0.4 T to prevent any harm to human tissues [184].

4.2. In vitro MDT models for intravenous drug delivery to the lungs

Due to the complexity of *in vivo* models for MDT drug delivery testing, several *in vitro* models have been developed to address the needs of MDT drug delivery modeling. These *in vitro* MDT models have been developed to examine different MN-drug compositions and delivery strategies with the aim of developing a predictive and less invasive MDT approach.

The implant-assisted (IA) MDT is considered as a practical approach to increase the retention of magnetic particles at the target site. Aviles et al. [185] designed an *in vitro* model of porous polyethylene (PE) polymer as the surrogate capillary tissue to investigate the delivery of dextran-coated magnetite particles under the influence of a magnetic field within the -1T to 1T magnetic strength. The effects of factors like diameter of the magnetic seeds and distance between the magnet and the membrane were studied. The magnetic seed of about 45.2% was achieved at a distance of 3 cm from the membrane, where the IA-MDT was used as a wire or stent. In another study, an *in vitro* MDT model of a glass tube containing the blood was employed by Nishijima et al. [186] to investigate the effect of magnetic force and drag force on an accumulation of ferromagnetic nanoparticles under the influence of a magnetic 4.5 T a. As a result, they succeed to locally accumulate particles in the blood flow located at a distance of 25 mm from the magnet source. Chuzawa et al. [187] further developed an *in-vitro* model of capillary vessels connected to the two columns of simulated organs to characterize the accumulation of MNPs in the deep part of the body under the effect of an external magnetic field. Also, a new MDT system was designed to simulate DOX-MNPs delivery in Lewis lung carcinoma (LLC) cell lines, where the drugs under the magnetic field resulted in a higher apoptosis rate [183].

4.3. Numerical simulation for simulating the intravenous MDT to the lungs

Computational fluid dynamic (CFD) methods have provided a great opportunity in predicting the fate of MNPs in the human body [60–63]. In many MDT investigations, experimental examinations are very expensive and testing of various scenarios is nearly impossible. Numerical simulations can provide a deep insight on effect of various MDT parameters such as particle diameter, flow rate of the blood in target vessels, position and strength of the magnet, gradient of the magnetic field, interaction of the particles and blood components, and trajectory of the particles in response to the magnet [65,188,189]. Manshadi et al. [56]

studied the effect of permanent magnet on the magnetic delivery of drug particles into artery tissues. For the first time, the four layers of the artery and their porosity were considered in the simulation to investigate the retention of drugs with the artery walls. Different parameters such as magnet size, particle size, drug/cargo size, and relative magnetic permeability were studied to optimize MDT through the artery wall. Cherry et al. [190] studied the effectiveness of permanent magnet for trapping magnetic particles flowing in the laminar blood flow in different arteries. The results showed that trapping the MNPs under the influence of Maxwell coil was more difficult in large arteries than in small ones. Moreover, the effect of parameters, such as blood flow velocity, drug particle size, and magnetic field strength, was assessed on the efficacy of MDT. In another study, controlling the swarm of magnetic particles was shown to increase the drug concentration and decrease the travel time of the particles in the target tissue [191]. Kumar et al. [192] further presented a physical-based model of MDT for drug delivery to an artery to optimize the path of a swarm of particles in the presence of a permanent magnet with 2 T magnetic field strength. Utilizing a magnetic field increased the number of particles with an increased scale of 6.4, demonstrating a promising outcome in the localization of particles inside tissues. Another model utilized a numerical simulation to characterize the response of magnetic nanoparticles in the aorta to a tree bar magnet (magnetization of each was =1.195 T). They estimated particle trajectories and retention of particles considering the key parameters of flow velocity and retention rate [193].

Numerical modeling was also employed to optimize the process of MDT. Kenjeres [194] included a non-uniform magnetic field (1–4 T) for different stenosis in a realistic model of right-coronary human arteries in which non-uniform magnetic field caused changes in the secondary flow pattern (a streamwise velocity contours deformed to perpendicular). In another study, the effect of Brownian motion and the interaction of red blood cells and super-paramagnetic nanoparticles were modeled in a Poiseuill flow [195]. The optimized size of nanoparticles was successfully steered to tumors with the size of up to 2 mm in diameter under the influence of an external magnetic field. The Brownian motion was shown to play a pivotal role in the trajectory of particles given its importance in modeling the diffusion of particles and their collisions with red blood cells.

Numerical simulation has also been used to design appropriate magnetic particles to guide drugs to a targeted zone [196]. Agiotis et al. [197] designed a magnetic carrier using Fe_3O_4 core for loading anticancer drugs to deliver the drugs to tumor cells. The effect of shape of electromagnet on magnetic drug targeting was studied and the results were in good agreement with the experimental data. Tip-top design, one side of the core, adopts a tip design in between the two face-to-face permanent magnet and provides the highest magnetic field strength for particle manipulation and field gradients for controling the orientation of particles.

More importantly, magnetization optimization has gained much interest to control the trajectory of particles by an individual or arrayed magnets [198,199]. Barnsley et al. [200] developed a numerical simulation and an *in-vitro* model to optimize the attraction of magnetic nanoparticles against a constant flow using a two-layer magnet array. This permanent magnet eases the disadvantages of other systems like Halbach arrays [201] to provide and modify magnetization without changing its physical dimension.

Given a practical challenge of employing a permanent magnet in some part of the body due to its large distance to the target site (5–10 cm), implanting an intravascular catheter would be a promising approach to deliver magnetic particles in the bloodstream [202]. Iacovacci et al. [203] developed an axisymmetric model of the bloodstream by considering the physical effects of fluidic drag force because of the blood flow, magnetic attraction due to the external magnet, and particle motion under the effect of the fluidic force and the magnetic field. This magnetic catheter consisting of 27 permanent magnets succeeded in both deployment and retrieving unused 500 and 250 nm

Table 4

Overview of the major types of MNPs and their compositions, advantages, and drawbacks. The second column of Table 4 summarizes the clinical utility of the MNPs as carriers for drug delivery to lung tumors and the corresponding clinical outcomes.

Magnetic nanoparticles	Compositions, advantages, and drawbacks	Clinical utility and outcomes
Iron oxide nanoparticles	*Composition* Colloidal iron oxide nanoparticles (SPIO and USPIO) typically composed of nanocrystalline magnetite (Fe3O4) or maghemite (γFe2O3) protected with coating [151]. *Advantages* excellent biocompatibility and biodegradability ease of synthesis *Disadvantages* variable magnetization vastly among synthesis methods even within particles of similar size due to incorporation of impurities disrupting the crystal structure toxicity due to ROS production non-specific targeting [152,153]	SPIONs were used for magnetic hyperthermia. A single magnetic hyperthermia regimen reduced the tumor growth [49]. Superparamagnetic iron oxide NPs (SPIONPs) with an average size of 10 ± 2 nm were coated with doxorubicin (Dox)-conjugated heparin (DH-SPIO) and used for targeted anticancer drug delivery. DH-SPIO NPs displayed a higher efficacy than Dox in inhibiting tumor growth and therapy of A549 human lung carcinoma [154].
Metallic nanoparticles	*Composition* made from iron, gold, cobalt, or nickel, often overlooked for biological applications due to their chemical instability. Iron nanoparticles: *Advantage* Iron nanoparticles possess high magnetization and are able to maintain super-paramagnetism at larger particle sizes compared to other oxide counterparts [155] *Disadvantages* 1- complex synthesis process 2- are typically protected by coatings, such as gold or silica to form a core-shell structure [156] Gold coatings: *Advantage* better biocompatibility and bioavailability, accumulate at tumor site & enhance x-ray effect *Disadvantage* stability related issue during aqueous formation [157]. silver magnetic nanoparticles: *Advantage* induced apoptosis in the targeted area, accumulation at the tumor site, and enhanced x-ray effect *Disadvantage* toxicity due to ROS production [158]	Papain-encapsulated and fluorouracil bio-conjugated gold NPs were synthesized while using papain as an anti-cancer. The efficacy of 5F-PpGNPs against human lung cancer A549 cell line improved significantly over that of pure 5-drug [159] A controlled synthesis of methotrexate (MTX) AgNPs using borohydride and citrate were utilized as reduction and reduction/capping agents, respectively. A significant performance against lung cancer cells (A-549) was reported [160].
Bimetallic (or metal alloy) nanoparticles	Composition Dual-functional nanoparticles made from hydroxyapatite with iron and platinum ions incorporation (Pt-Fe-HAP) *Advantage* These MNPs exhibit super-paramagnetic properties. stable in biologically relevant media such as PBS the ability these MNPs to bind DNAs and proteins	Applicable for chemo-hyperthermia Pt-Fe-HAP was shown to be highly toxic to A549 cells after magnetic field treatment under hyperthermia but no damage to fibroblast cells was observed [161]. Recent advances in the synthesis of FePt nanoparticles have made these MNPs an option of choice for biomedical applications. The nteraction between the two chemical species in these NPs leads to a greater chemical stability in comparison with other high moment metallic nanoparticles [162].
Co-polymer modified magnetic nanoparticles	*Composition* coating of MNPs with polymers is the most common way to solve the stability issue of nanoparticles against oxidation [163,164]. *Advantages* suitable carrier for a hydrophobic therapeutic agent *Disadvantages* non-specific targeting [165] drug delivery via chitosan coated Fe_2O_3 MNPs in vitro could be improved if the drugs were modified with antibodies, proteins, or ligands [166].	EGRF-PLGA MNPs were used for drug delivery system where drug-loaded MNPs reduced the number of viable A549 cells significantly [167]. Silibinin-loaded PLGA-PEG-Fe3O4 nanoparticles was used where an enhanced inhibitory effect on the growth of A549 lung cancer cell line and hTERT gene expression was detected in compared to pure Silibinin [168]. mesoporous silica nanoparticles (MSNs) was conjugated to polymer matrix acting as drug container to enhance the drug encapsulation efficacy. Methotrexate (MTX) used as a model drug was successfully loaded in MNCs (M-MNCs) with promising dose-dependent anticancer efficacy against A548 cell [169]. dextran-coated magnetite seed particles increased the capturing efficiency of magnetic drug carrier particles in capillary tissues [170]. Fe_3O_4 nanoparticles coated with Polyethylene Glycol (PEG) promoted water solubility, reduced toxicity, decreased enzymatic degradation and increased the in vivo half-lives of small molecule drugs during their magnetic drug delivery [171] [172].

SPIONs from the bloodstream. In a more advanced simulation, the interaction of paramagnetic nanoparticles with each other due to an external magnetic field in the realistic model of the central blood distribution system was modeled using the Lattice-Boltzmann method in a three-dimensional vascular system [204]. The study focused on assessing the density of the particles in a targeted site in the Willis vascular system. Different parameters were optimized, such as the effect of coating thickness, impact of gravity, and magnetic properties of the

particles. For instance, no difference is observed due to the coating or gravity for large particle size. Also, the size and crystallinity of super-magnetic particles were determined for particles with radius larger than 65 nm to achieve the maximal magnetic susceptibility.

Despite many numerical studies on MDT in the bloodstream focusing MDT in the brain and heart, there is no report of theoretical modeling of MDT in the lung cancers, where drugs are intravenously delivered to the body. The in vivo, in vitro, and numerical models

Table 5
Overview of the studies on intravenous magnetic drug targeting of the lungs (In vivo, in vitro and numerical models)

Testing method	Drugs	Type & magnetic field strength	Outcome	Authors, year
In vivo	30 nm Doxorubicin magnetite nanoparticle conjugates (DOX-M)	A stationary magnetic field of 0.2 T	Considerable accumulation in the lungs	Mykhaylyk et al., 2005 [179]
	250 nm dextran-coated Fe_3O_4 NPs	NdFeB permanent magnet (with a maximum magnetic flux density of 2.4 kG)	No influence in the lungs but influential on the liver and spleen	Wu et al., 2007 [180]
	DOX-loaded magnetic gold nanoparticles (MGNPs- 99 DOX)	N.A 1.14 T	Higher accumulation in the presence of a magnet compared to the no-magnet test	Elbialy et al., 2015 [181]
	Iron oxide nanoparticles (MNPs)	Permanent magnet 1080–1150 mT	Combining the magnetic field and ultrasound makes the accumulation 2 to 3 folds higher than a passive system.	Vlaskou et al., 2010 [182]
In vitro	MNPs and DOX-MNPs	A disk magnet -0.5 T	Enhancing the antitumor activity	[183]
	Dextran- coated magnetic particles	An implant-assisted magnetic -1T to 1T	Decreasing the distance of magnet, increase of the seed particle diameter, and increasing the seed suspension injection volume cause the capture of particles more	Aviles et al., 2009 [185]
	Ferromagnetic nanoparticles	Bulk superconducting magnet magnet 0.1 T/m to 100 T/m	Nanoparticles accumulated successfully in blood flow with 20 mm distance from the magnet	Nishijima et al, 2007 [186]
	MNPs	Permanent magnet > 0.7 T	Enhancing the local accumulation in the deep lungs	Chuzawa et al., 2011 [187]
Numerical	DOX-MNPs	A disk magnet 0.5 T	Higher apoptosis rate in the lungs	Jia et al, 2012 [183]
	N.A			

N.A: not available

---

developed for intravenous magnetic drug targeting of the lungs are summarized in Table 4.

5. Magnetic drug delivery to lung tumors through the respiratory system

In addition to the intravenous injection of drugs and their delivery to the lungs, researchers and clinicians have demonstrated lung disease therapy using inhalational nanomedicine particles. The MDT, through the respiratory system, is one of the promising approaches to enhance local drug concentration for the treatment of lung diseases [205]. Here, we classified these studies in three subsections of *in vivo* and *in vitro* experiments as well as numerical simulations (Table 6).

5.1. In vivo MDT models for respiratory drug delivery to the lungs

Monitoring the deposition of aerosol particles in an animal's lungs have provided scientists with insights on lung diseases [206–210]. This delivery route has also been used for MNP-based anticancer drug delivery to the lungs under stimulation of external magnetic fields. Dames et al. [211] used SPIONs loaded in aerosol droplets and nebulized them to the lungs of mice by the use of wire coil producing a magnetic field. The magnetic field accumulated the SPIONs in central airways or lung periphery rather than local regions. Sadhuka et al. [212] produced MNPs for targeted hyperthermia in lung cancer in a mouse orthotopic model of NSCLC, where the targeted SPIONs inhibited lung tumor growth. Price et al. [213] demonstrated magnetic-based drug localization in the lungs, showing a 10-fold increase in magnetic microparticle (doxorubicin-loaded) concentration deposited in specific regions of the lungs. In another study, drug-loaded MNPs were coated with polylactic-co-glycolic (PLGA) to avoid drugs from aggregation in mice and to enhance their uptake into lung carcinoma cells [214]. Hasenpusceh et al. [215] introduced drug-loaded SPIONs via the respiratory system where they demonstrated the 3-fold increase in trapping efficiency of these NPs in the presence of a magnet applicable for curing deeper airways. Magnetic fields were also employed in form of an implantable stimulating system to force aerosols into alveoli of pegs for the treatment of lung cancers [216]. Xie et al. [217] used oleic acid-coated magnetic particles to target drug deposition in the trachea of mice. They reported a twice increase in the deposition rate of aerosol particles throughout the airways.

### 5.2. In vitro MDT models for respiratory drug delivery to the lungs

In vitro MDT experiments have also been utilized for targeted delivery of aerosol particles carrying chemotherapeutic agents [218]. Magnetic gradient of 3 T/m was employed to steer particles inside the acrylic channel where the permanent magnet was positioned underneath the agar layer to quantify particles in the channel. Also, the trapping efficiency of MNPs was reported between 48%–87%. Martin and Finlay [219] developed an *in vitro* bifurcation airways platform utilizing permanent neodymium magnets to measure trapping efficacy of aerosol drug particles. The results demonstrated 1.74 higher deposition of aerosols (by mass) in the presence of a 55 mT magnet field compared to no-magnet state. Xie et al. [220] compared the data of *in-vitro* and CFD models for further analysis of drug inhalation applicable for treatment of lung cancers. In their experimental model, a glass tube was built to investigate the deposition of magnetite nanoparticles in the presence of a 0.4 T wedge-shaped permanent magnet, where the magnet was placed at a distance of 3 mm above the tube. They studied the impact of different parameters such as particle size, flow rate, and tube diameter on particle deposition. This MDT study enabled to increase the particle deposition by 71%. In other *in vitro* lung cancer studies, Upadhyay et al. [221] used SPIONS coated with lipid microparticles under a 0.2 T magnetic field in an *in vitro* system for gentle drug release in an inhalable drug delivery model without any harmful

Table 6
Overview of various studies on pulmonary magnetic drug delivery to lung cancers/tumors.

Method	Magnetic micro or nano particles	Types & strength of magnet	Outcome	Authors, year
In vitro, CFD	1–3 μm carbonyl iron	Permanent magnet-36- 45 mT	Trapping of 48-87% of MNs	Ally et al., 2005 [218]
In vivo, CFD	80 nm SPION	Wire core- magnetic flux gradient of > 100 T/m	Accumulation in central airways rather than the local regions	Dames et al., 2007[211]
In vitro	Magnetite-loaded Cromoglicic acid aerosols Nanoparticles	Permanent magnet-50-60 mT	Increased deposition by a factor of 1.74 (by mass)	Martin and Finlay, 2008 [219]
In vivo	Oleic acid-coated magnetite particles	NA	NA	Dahmani et al.,2009 [216]
In vivo, in vitro	0.3-4.5 μm iron oxide	Permanent magnet-2.3-3.3 T	Increased deposition fraction from 0.25 to 0.57	Xie et al., 2010 [217]
In vitro, CFD		Wedge- shaped magnet- 0.4 T	71.7% increase in deposition fraction	Xie et al., 2010 [220]
In vivo	200 nm SPIONs	Permanent magnet-0.2 T	3- fold increase in trapping efficacy	Hasenpusch et al., 2012 [215]
In vivo	2-4 μm SPIONS coating with lipid microparticles	Permanent magnet-0.21 T	100% trapping efficacy of SPIONSs	Upadhyay et al., 2012 [221]
CFD	minor diameter of 0.5 μm cromoglycic acid particles	NA	Increased local delivery by a factor of 1.43-3.46	Martinez et al., 2013 [224]
In vivo	369 nm SPIONs	Magnetic hyperthermia with a nominal magnetic field strength of 6 kA/m	Enhancement in tumor retention of SPIONs	Sadhukha et al., 2013[212]
In vivo, In vivo	54.3 nm & 293.4 nm PLGA[a]-MNP	NA	NA	Verma et al., 2013 [214]
In vitro	2.8 μm SPIONs loaded Trojan porous	Permanent magnet-NA	4-fold increase in particle deposition	Tewes et al., 2014 [222]
CFD	2-6 μm Doxorubicin	Non-uniform magnetic field-4.043 T	100% particle trapping	Pourmehran et al., 2015 [225]
In vitro	Nanoparticles iron oxide	The field strength of approximately 55 kA/m	NA	Stocke et al., 2015 [223]
CFD	2-6 μm Doxorubicin	Wire core- magnetic field strengths ≤ 1.5 T	100% drug trapping	Pourmehran et al., 2016 [226]
CFD	0.5-3 μm SPION	Permanent magnet-0.43 T	Particle deposition increased from 40% to 100%	Ostrovski et al., 2016 [228]
In vivo	3.2 μm NIMs SPION	Permanent magnet-0.58 T	14-40% increase in particle trapping	Price et al., 2017 [213]
CFD	0.1-10 μm iron oxide-maghemite core	NA-2 T	20-85% increase in particle deposition	Kenjeres and Tjin, 2017 [229]
CFD	5 nm gold/iron-oxide	Rectangular coil-46.21 mT	0.3% decrease in particle trapping	Russo et al., 2017 [230]
CFD	0.25-2 μm Fe$_3$O$_4$	Current carrying wire-1.432 T	4-fold increase in deposition efficiency	Mohammadian and Pourmehran, 2019 [231]
CFD	0-2 μm SPIONs	Cylindrical permanent magnet-1.4T	0.5–35% increase in deposition fraction	Nikookar et al., 2019 [232]
CFD	5-9 nm MNPs	Coil-10-20 A	2% increase in deposition in tumor	Sabz et al., 2019 [205]
CFD	1-7 μm MNPs	Permanent magnet-0.25–1.2T	Deposition fraction increased 68%	Manshadi et al., 2019 [233]

N.A.: not available

[a] polymer poly (lactic-co-glycolic acid)
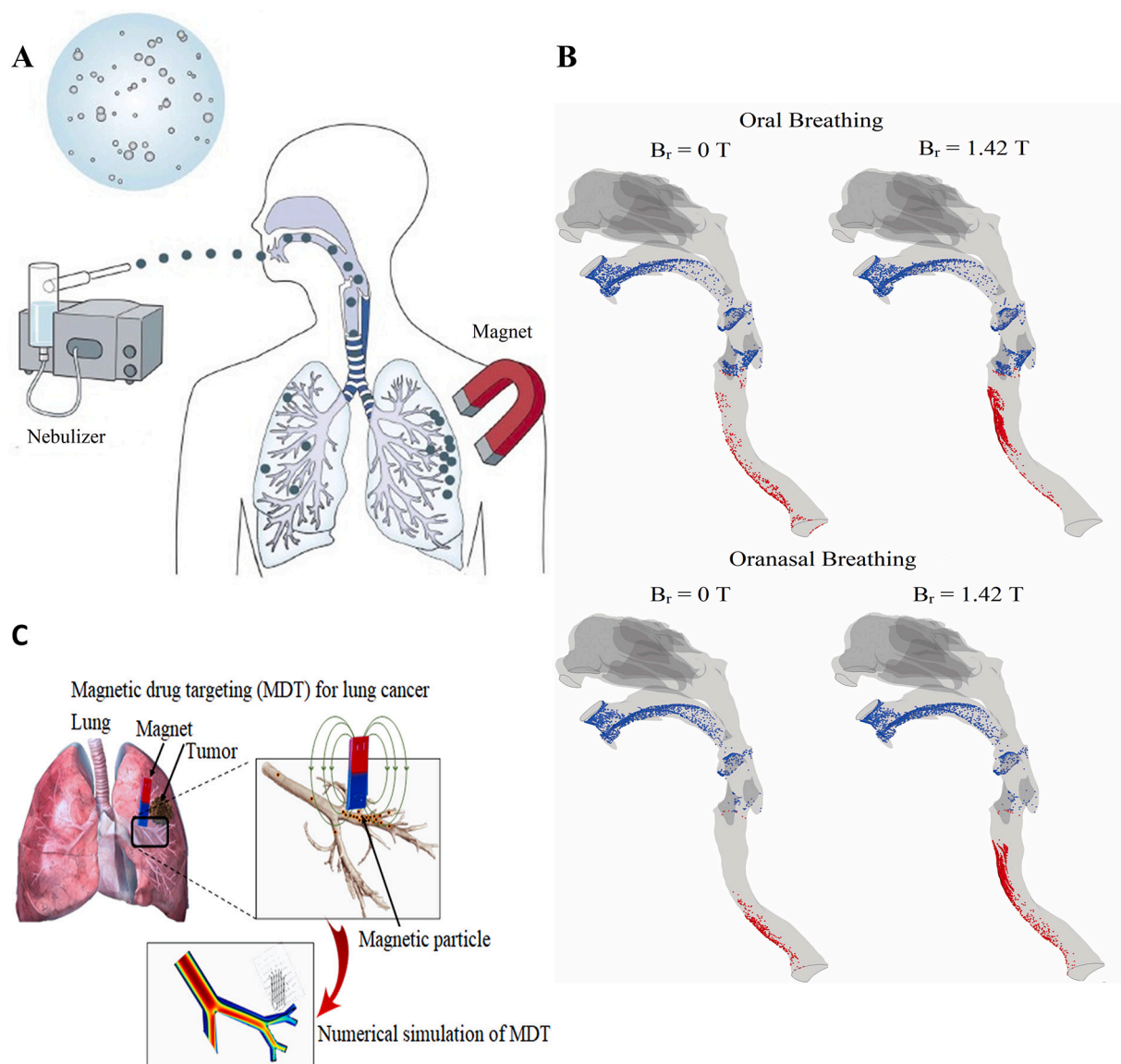
Fig. 2. Respiratory magnetic drug delivery in lung cancers [38]. A) Magnetic drug targeting of aerosol particles via the respiratory system [38]. B) Particle trapping under the influence of different magnetic fields for oral and oranasal breathing [232]. C) Mechanism of magnetic aerosol drug targeting (MADT) in lung cancer [233].

side-effect. The efficiency of trapping of the aerosol drugs was demonstrated to be 100%. Sometimes NPs cause aerosolization in the lungs because of their high density, therefore researchers employed SPIONs-loaded Trojan for magnetic targeting in order to enable tracing of the aerosols [222]. A combination of SPIONs, PEG, and hydroxypropyl-β-cyclodextrin (HPβCD) formulated the Trojan microparticles and facilitated drug targeting in the lungs under the effect of a magnetic field. The other *in vitro* study focused on exploiting magnetic nanocomposite microparticles (MnMs) combined with the MNPs and D-mannitol drug [223]. Given the easy exhale of MNPs from lungs due to their small size, MNPs were loaded into magnetic particles while D-mental was used for hyperthermia therapy. Also, preparation of these drugs with aqueous co-precipitation further increased the deposition of particles in the lungs.

5.3. Numerical simulation of MDT models for respiratory drug delivery to the lungs

Xie et al. [220] used numerical simulations to predict particle deposition of a previously studied *in vitro* MDT model by employing the

wedge-shaped permanent magnet (The magnet placed at a distance of 2 mm). The numerical model was used to study effect of different parameters such as flow rate, tube diameter, and particle size on the efficacy of particle deposition. The larger the diameter of particles, the higher the efficacy of deposition fraction. In addition, increasing the flow rate and tube diameter enhanced the deposition fraction. The experimental results were found to be in good agreement with the CFD simulation data. In another study, Martinez et al. [224] developed a CFD model to study drug delivery through deep down airways by ellipsoidal magnetic particles, where the results showed that the presence of the magnetic increases local enhancement in drug delivery by a factor of 1.43–3.46 in symmetrical bronchial bifurcation. Pourmehran et al. [225] presented a CFD model of a realistic lung model (G0-G2) to investigate deposition efficiency under the influence of non-uniform magnetic field. Purmehran et al. [226] simulated a deep respiratory region in which the effect of a permanent magnet, magnet position, and inhalation flow rate on particle deposition was studied. For the magnetic field strengths of below 1.5 T, the deposition efficiency was enhanced by increasing the particle size. However, for magnetic field strengths of above 1.5 T, the deposition efficiency decreased by

increasing the particle size. The premier study of Kraficik et al. [227] investigated the effect of a quadrupole magnetic field on the steering of aerosolized magnetic nanoparticles into the alveolar region. In another research, Ostrovski et al. [228] simulated the deposition of SPION in a deep site of acinus under the effect of a permanent magnet. Placing the magnet closer to the acinar region enhanced the magnetic field strength and therefore improved the deposition efficiency from 40% to 100%. Kenjeres et al. [229] developed a CFD model to simulate a real human lung from mouth to the eighth generation of a bronchial branch under the delivery of iron oxide-maghemite core. The magnetic stimulation of these particles increased the deposition efficiency for about 85%, demonstrating the applicability of MDT approaches for the treatment of respiratory diseases. In another study, therapeutic performance of magnetic nano-drug targeting using a rectangular coil as an external magnet was studied on a realistic model of the trachea [230]. As a result, the deposition of aerosol particles reduced from 50% to 47% by imposing a magnetization field. The study design was not therefore effective to improve drug delivery, highlighting the needs to selection of appropriate design parameters. Another CFD model of respiratory airway tree was simulated to investigate targeted drug delivery of Fe_3O_4 particles under the influence of an external magnetic field (1.43 T) [231]. The results show a 4-fold increase in deposition efficiency. Nikookar et al. [232] simulated a mimetic model of upper airway and trachea, where they studied the influence of drug composition, air-breathing condition, position of magnet, and angle of the magnetic source on particle deposition. The results showed about 75% deposition efficacy of 8 μm magnetic particle size at 5 L/min airflow rate. Also, the optimal angel of the magnetic source was estimated to be 0˚ when the patient lie on his/her back (Fig. 2B).

A few CFD studies have been conducted specifically to simulate MDT performance in lung tumors. Sabz et al. [205] investigated the MDT in lung cancer in the upper airways by using a coil to produce a magnetic field. In the following study, we simulated the lung cancer model in the airways (G0-G3) and used a permanent magnet to steer magnetic drug particles toward tumors [233] (Fig. 2B). The effect of parameters such as permeability, magnet size, magnet position, and magnetic field strength on drug delivery was studied. The results show that implementing a permanent magnet near the G0 resulted in 49% trapping of 7 μm particles. Moreover, increasing the magnet size (H = 4 cm, D = 2 cm) contributed to 75.8% particle deposition fraction. Furthermore, an increase in magnetic field strength from 0.25 to 1.25 T enhanced the delivery from 5.7% to 34% for 7 μm MNPs (Fig. 2C). The summary of these numerical studies is detailed in Table 6.

6. Challenges and future perspectives

The field of magnetic particle delivery has demonstrated considerable advances in clinical practices. Magnetic particle targeting is prone to be the most significant technological advances owing to its less invasive treatment and highly efficient targeted drug delivery. However, several challenges still need to be addressed to facilitate its diagnostic and treatment utility for lung cancers. Also, researchers need to further evaluate its therapeutic efficiency and identify clinical risks.

Utilizing proper imaging techniques like PET and DWI creates detailed images applicable for better lung cancer detection. Also, a combination of these imaging techniques with MRI facilitates diagnosis of lung cancers due to much higher sensitivity and specificity in detecting metastatic nodes [234,235]. MRI plays a leading role in the diagnosis of NSCLC's stages.

Magnetic particle targeting approaches in lung cancers involves intravascular injection and pulmonary system, employed so far in the lungs, liver, and spleen *in vivo* and *in vitro* models. The permanent magnet is the most effective method to steer drugs to particular tissues without being aggregated in healthy tissue. However, in most of these studies, steering drugs in non-targeted tissues has not yet been considered. Further computational or biomimetic *in vitro* models (using

multiorgan-on-chip technologies [236]) of MDTs could facilitate understanding of how MNPs may be absorbed into other healthy tissues like the brain and heart.

Several investigations have reported the utility of magnetic drug delivery into lung cancers through the respiratory system, which demonstrates the high capability of the magnetic field in steering drugs to the desired region of the lungs. However, the proper design of magnetic field strength and the appropriate location of the permanent magnet needs further systemic investigation. Furthermore, numerical simulations have provided primary insight about the effect of various design parameters in the deposition fraction of MNPs using a permanent magnet, although there are still limitations in simulating complex but biomimetic models. Further advances in developing complex 3D CFD models of different lung cancers and MDT models could position the numerical MDT models as a predictive system for system design prior to proceeding to *in vitro* and *in vivo* experiments.

More importantly, one of the global concerns these days is the severe acute respiratory syndrome coronavirus 2 (COVID-19), which has no specific medication recommended hitherto [237]. Although a few drug candidates were recently considered by FDA for COVID-19 treatment, there is a certain need to facilitate finding effective therapeutic agents to inhibit the production of virus particles, block the receptors, and/or develop vaccine [237,238]. In this context, an excellent drug delivery technique like MDT might be a promising alternative to overcome passive transfer of candidate drugs and therefore elevate cellular uptake, enhance permeability and efficacy, decrease expenses, and reduce the complexity of pathology to address the needs of pandemics.

7. Conclusion

The respiratory system is the main entrance for nanoparticles due to the large surface area in contact with the outside environment (about 143 ± 12 m^2 alveolar surface area with about 2.2 μm structural barrier between the air and the blood). This huge gateway is exposed to different environmental materials through inhalation and systemic administration, which results in activation of various defense mechanisms (e.g., dendritic cells, surfactant, secretory immunoglobulins, alveolar macrophages, and mucociliary escalator) in the lung [239]. Vulnerable lung tissues are also affected by different disease conditions like cancer. Lung cancer is the third cause of death worldwide and needs new diagnostic and treatment strategies to cure. Compared to conventional strategies for lung cancer treatment, magnetic drug targeting (MDT) presents new potential for lung cancer treatment where drug delivery to the lungs is aided by magnetic particles subject to external magnetic force. MDTs have been effective in target drug delivery due to their inherent characteristics such as deliberate control on drug concentrations, increased efficiency of drug targeting, low treatment cost, and much fewer side effects to healthy tissues. Two major routes of MDT implementations are intravenous injection and respiratory system. Most of the studies have so far focused on the pulmonary drug delivery system rather than intravenous injection due to its great outcomes in local delivery as well as high absorption of large molecules into airway circulation. Numerical models of MDTs have shown superior performance in predicting *in vitro* and *in vivo* MDT models and are expected to be strong MDT models for the development of *in vivo* MDT strategies.

Medical imaging systems like CT- scan or chest X-ray have been utilized to detect zones of the lung with more opacity. Opacity can be conferred as lung cancer, pneumonia, infiltration, or calcification of lung parenchyma. In symptomatic patients with COVID-19 or other viral respiratory tract infections who suffer from dyspnea, cough, or low oxygen saturation, imaging methods can be used to detect opacified lesions on lung parenchyma. For example, the CT imaging presentations of novel coronavirus pneumonia (NCP) are mostly patchy ground-glass opacities in the peripheral areas under the pleura with partial consolidation. Once improved, they are detected by the signature of fibrotic

stripes [240]. Magnetic drug delivery systems have been offered to deliver therapeutic agents to the inflamed lung tissue more efficiently and with fewer side effects. Magnetic nanoparticle-coated drugs can be administered as either spray or injection, where the magnet can be placed next to the lesion. This strategy can lead to a more efficient treatment and clinical prognosis. Also, computational fluid dynamics could be utilized to determine appropriate particle size, location of magnet, spray velocity, and dosing, for effective therapies for pulmonary viral infectious diseases like COVID-19 [241].

Although MNPs have a large number of potential therapeutic use in various diseases, there are still limitations in implementing magnetic particle delivery systems. The primary challenge is related to the toxicity of MNPs, which needs detailed evaluation for any new particle or even formulation. This matter has been meticulously studied by researchers in this field though only for specific types of MNPs (e.g., MNP accumulation, inflammatory reactions, oxidative stress, increases in microvascular permeability, and chronic iron toxicity [242]) in the lung [27–30,35]. The other limitation of using MNPs is relevant to the high strength of the external magnetic field applied to manipulate MNPs and capture the NPs in the location of interest. The geometry and the distance of the magnet source is crucial to regulate their capability to manipulate NPs. To address this issue, employing of a permeant magnet inside or outside the body has been computationally suggested [56,185,201,233,242]. Further *in vivo* studies need to be implemented to identify the potential utility of a permanent magnet for effective magnetic drug delivery. In addition, the size and particle material are also important and these two characteristics of particles need to be adjusted to avoid magnetic agglomeration wherever the magnetic field is removed [64,243,244]. Besides, most of investigations in this field have been so far applied on animals. However, challenges may arise once these methods are examined in human due to the physiological differences [245,246]. Last but not the least, the MDT methods have been shown a level of success in well-defined tumors. Further investigation is needed to examine their utility for metastatic neoplasms and small tumors in the early stages.

Further advances in developing new magnetic particle drug delivery methods could not only contribute significantly to the diagnosis and treatment of lung cancers but also other lung infectious diseases and acute respiratory syndromes, including COVID-19, MERS, and SARS.

References

[1] S.H. van Rijt, T. Bein, S.J.E.R.J. Meiners, Medical nanoparticles for next generation drug delivery to the lungs, Eur. Respir. J. 44 (2014) 765–774 erj02128-02013.

[2] F. Bray, J. Ferlay, I. Soerjomataram, R.L. Siegel, L.A. Torre, A. Jemal, Global Cancer Statistics 2018: GLOBOCAN estimates of incidence and mortality worldwide for 36 cancers in 185 countries, CA Cancer J. Clin. 68 (2018) 394–424.

[3] R.L. Siegel, K.D. Miller, A. Jemal, Cancer statistics, 2019, CA Cancer J. Clin. 69 (2019) 7–34.

[4] C. Gridelli, A. Rossi, D.P. Carbone, J. Guarize, N. Karachaliou, T. Mok, F. Petrella, L. Spaggiari, R. Rosell, Non-small-cell lung cancer, Nat. Rev. Dis. Primers. 1 (2015) 15009.

[5] G.P. Kalemkerian, Small cell lung cancer, Seminars in respiratory and critical care medicine, Thieme Medical Publishers, 2016, pp. 783–796.

[6] R.L. Riegel, K.D. Miller, A. Jemal, Cancer Statistics, 2017, 67 (2017), pp. 7–30.

[7] I. Sekine, M. Sumi, M. Satouchi, K. Tsujino, M. Nishio, T. Kozuka, S. Niho, K. Nihei, N. Yamamoto, H.J.Cs. Harada, Feasibility study of chemoradiotherapy followed by amrubicin and cisplatin for limited-disease small cell lung cancer, Cancer Sci. 107 (2016) 315–319.

[8] A. Argiris, J. Murren, Staging and clinical prognostic factors for small-cell lung cancer, Cancer J. 7 (2001) 437–447.

[9] I. Demedts, K. Vermaelen, J. Van Meerbeeck, Treatment of extensive-stage small cell lung carcinoma: Current status and future prospects, Eur. Respir. J. 35 (2010) 202–215.

[10] M. Noguchi, Y. Shimosato, The development and progression of adenocarcinoma of the lung, Lung Cancer, Springer, 1994, pp. 131–142.

[11] T. Ishizumi, U. Tateishi, S. Watanabe, Y. Matsuno, Mucoepidermoid carcinoma of the lung: High-resolution CT and histopathologic findings in five cases, Lung Cancer 60 (2008) 125–131.

[12] S.E. Weinberger, B.A. Cockrill, J. Mandel, Principles of Pulmonary Medicine E-Book, Elsevier Health Sciences, 2017.

[13] M.R. Davidson, A.F. Gazdar, B.E. Clarke, The pivotal role of pathology in the management of lung cancer, J. Thorac. Dis. 5 (2013) S463.

[14] M. Alfonse, M.M. Aref, A. Salem, An ontology-based system for cancer diseases knowledge management, Int. J. Inform. Eng. Elect. Busin. 6 (2014) 55–63.

[15] M. Sasaki, Y. Ichiya, Y. Kuwabara, Y. Akashi, T. Yoshida, T. Fukumura, S. Murayama, T. Ishida, K. Sugio, K. Masuda, The usefulness of FDG positron emission tomography for the detection of mediastinal lymph node metastases in patients with non-small cell lung cancer: a comparative study with X-ray computed tomography, Eur. J. Nucl. Med. 23 (1996) 741–747.

[16] K.W. Yong, J.R. Choi, M. Mohammadi, A.P. Mitha, A. Sanati-Nezhad, A. Sen, Mesenchymal stem cell therapy for ischemic tissues, Stem Cells Int. 2018 (2018) 1–11.

[17] N. Anjuman, N. Li, M. Guarnera, S.A. Stass, F. Jiang, Evaluation of lung flute in sputum samples for molecular analysis of lung cancer, Clin. Transl. Med. 2 (2013) 15.

[18] R. Zimmermann, Nuclear medicine: Radioactivity for diagnosis and therapy, EDP Sciences, 2019.

[19] A. Berger, How does it work? Magnetic resonance imaging, Br. Med. J. 324 (2002) 35.

[20] F. Laurent, M. Montaudon, O. Corneloup, CT and MRI of lung cancer, Respiration 73 (2006) 133–142.

[21] J.R. Molina, P. Yang, S.D. Cassivi, S.E. Schild, A. Adjei, Non-small cell lung cancer: epidemiology, risk factors, treatment, and survivorship, Mayo Clinic Proceedings, Elsevier, 2008, pp. 584–594.

[22] N. O'Rourke, M.R. i Figuls, N.F. Bernadó, F. Macbeth, Concurrent chemoradiotherapy in non-small cell lung cancer, Cochrane Database Syst Rev. 6 (CD002140) (2010).

[23] H.C. Fernando, A. De Hoyos, R.J. Landreneau, S. Gilbert, W.E. Gooding, P.O. Buenaventura, N.A. Christie, C. Belani, J. Luketich, Radiofrequency ablation for the treatment of non-small cell lung cancer in marginal surgical candidates, J. Thorac. Cardiovasc. Surg. 129 (2005) 639–644.

[24] C. Zappa, S. Mousa, Non-small cell lung cancer: Current treatment and future advances, Transl. Lung Cancer Res. 5 (2016) 288.

[25] A.C. Society, Non-small cell lung cancer survival rates, (2016).

[26] T.A. Baudino, Targeted cancer therapy: The next generation of cancer treatment, Curr. Drug Discov. Technol. 12 (2015) 3–20.

[27] A. Bahl, D. Sharma, P. Julka, G. Rath, Chemotherapy related toxicity in locally advanced non-small cell lung cancer, J. Cancer Res. Ther. 2 (2006) 14.

[28] A. Bircan, B. Berktaş, H. Bayız, N. Başay, S. Bircan, M. Berkoğlu, Effects of chemotherapy on quality of life for patients with lung cancer, Turk. Resp. J. 4 (2003) 61–66.

[29] A. Bezjak, C.W. Lee, K. Ding, M. Brundage, T. Winton, B. Graham, M. Whitehead, D.H. Johnson, R.B. Livingston, L. Seymour, Quality-of-life outcomes for adjuvant chemotherapy in early-stage non-small-cell lung cancer: Results from a randomized trial, J. Clin. Oncol. 26 (2008) 5052.

[30] J.-P. Chen, Y. Lo, C.-J. Yu, C. Hsu, J.-Y. Shih, C.-H. Yang, Predictors of toxicity of weekly docetaxel in chemotherapy-treated non-small cell lung cancers, Lung Cancer 60 (2008) 92–97.

[31] O. Taratula, O.B. Garbuzenko, A.M. Chen, T. Minko, Innovative strategy for treatment of lung cancer: Targeted nanotechnology-based inhalation co-delivery of anticancer drugs and siRNA, J. Drug Target. 19 (2011) 900–914.

[32] H. Koyama, Y. Ohno, S. Seki, M. Nishio, T. Yoshikawa, S. Matsumoto, K. Sugimura, Magnetic resonance imaging for lung cancer, J. Thorac. Imaging 28 (2013) 138–150.

[33] M. Kanamala, W.R. Wilson, M. Yang, B.D. Palmer, Z.J.B. Wu, Mechanisms and biomaterials in pH-responsive tumour targeted drug delivery: A review, Biomaterials 85 (2016) 152–167.

[34] N. Ullah, S. Noreen, K. Tehreem, A. Zaman, Z. Ahmad, H. Balouch, N. Samad, Liposome as nanocarrier: Site targeted delivery in lung cancer, Nanomedicine 8 (8) (2014) 1–32.

[35] S.A.A. Rizvi, A.M. Saleh, Applications of nanoparticle systems in drug delivery technology, Saudi Pharm J 26 (2018) 64–70.

[36] C. Sun, J.S. Lee, M. Zhang, Magnetic nanoparticles in MR imaging and drug delivery, Adv. Drug Deliv. Rev. 60 (2008) 1252–1265.

[37] V.P. Torchilin, Passive and active drug targeting: Drug delivery to tumors as an example, Drug Delivery, Springer, 2010, pp. 3–53.

[38] C. Kleinstreuer, Y. Feng, E. Childress, Drug-targeting methodologies with applications: A review, World J. Clin. Cases: WJCC 2 (2014) 742.

[39] L.E. van Vlerken, T.K. Vyas, M.M.J.P.r. Amiji, Poly (ethylene glycol)-modified nanocarriers for tumor-targeted and intracellular delivery, Pharm. Res. 24 (2007) 1405–1414.

[40] W. Song, M. Li, Z. Tang, Q. Li, Y. Yang, H. Liu, T. Duan, H. Hong, X. Chen, Methoxypoly (ethylene glycol)-block-Poly (L-glutamic acid)-loaded cisplatin and a combination with iRGD for the treatment of non-small-cell lung cancers, Macromol. Biosci. 12 (2012) 1514–1523.

[41] T. Yang, D. Nyiawung, A. Silber, J. Hao, L. Lai, S. Bai, Comparative studies on chitosan and polylactic-co-glycolic acid incorporated nanoparticles of low molecular weight heparin, AAPS PharmSciTech 13 (2012) 1309–1318.

[42] E. Gullotti, Y. Yeo, Extracellularly activated nanocarriers: A new paradigm of tumor targeted drug delivery, Mol. Pharm. 6 (2009) 1041–1051.

[43] P. Dames, B. Gleich, A. Flemmer, K. Hajek, N. Seidl, F. Wiekhorst, D. Eberbeck, I. Bittmann, C. Bergemann, T. Weyh, Targeted delivery of magnetic aerosol droplets to the lung, Nat. Nanotechnol. 2 (2007) 495.

[44] Z. Wang, R. Qiao, N. Tang, Z. Lu, H. Wang, Z. Zhang, X. Xue, Z. Huang, S. Zhang, G. Zhang, Active targeting theranostic iron oxide nanoparticles for MRI and magnetic resonance-guided focused ultrasound ablation of lung cancer, Biomaterials 127 (2017) 25–35.

[45] M. Li, W. Song, Z. Tang, S. Lv, L. Lin, H. Sun, Q. Li, Y. Yang, H. Hong, X. Chen,

Nanoscaled poly (L-glutamic acid)/doxorubicin-amphiphile complex as pH-responsive drug delivery system for effective treatment of nonsmall cell lung cancer, ACS Appl. Mater. Interfaces 5 (2013) 1781–1792.

[46] D.-K. Chang, C.-T. Lin, C.-H. Wu, H.-C. Wu, A novel peptide enhances therapeutic efficacy of liposomal anti-cancer drugs in mice models of human lung cancer, PLoS One 4 (2009).

[47] K.M. Pondman, N.D. Bunt, A.W. Maijenburg, R.J. van Wezel, U. Kishore, L. Abelmann, E. Johan, B. Haken, Magnetic drug delivery with FePd nanowires, J. Magnet. Mag. Mater. 380 (2015) 299–306.

[48] Q.A. Pankhurst, J. Connolly, S.K. Jones, J. Dobson, Applications of magnetic nanoparticles in biomedicine, J. Phys. D Appl. Phys. 36 (2003) R167.

[49] T. Sadhukha, T.S. Wiedmann, J. Panyam, Inhalable magnetic nanoparticles for targeted hyperthermia in lung cancer therapy, Biomaterials 34 (2013) 5163–5171.

[50] J. Ally, B. Martin, M.B. Khamesee, W. Roa, A. Amirfazli, Magnetic targeting of aerosol particles for cancer therapy, J. Magnet. Mag. Mater. 293 (2005) 442–449.

[51] M. Saadat, A.S. Goharrizi, Magnetic drug targeting to lung tracheal region.

[52] S.A. Rizvi, A.M. Saleh, Applications of nanoparticle systems in drug delivery technology, Saudi Pharm. J. 26 (2018) 64–70.

[53] H.M. Abdelaziz, M. Gaber, M.M. Abd-Elwakil, M.T. Mabrouk, M.M. Elgohary, N.M. Kamel, D.M. Kabary, M.S. Freag, M.W. Samaha, S.M. Mortada, Inhalable particulate drug delivery systems for lung cancer therapy: Nanoparticles, microparticles, nanocomposites and nanoaggregates, J. Control. Release 269 (2018) 374–392.

[54] W.H. Lee, C.-Y. Loo, M. Ghadiri, C.-R. Leong, P.M. Young, D. Traini, The potential to treat lung cancer via inhalation of repurposed drugs, Adv. Drug Deliv. Rev. 133 (2018) 107–130.

[55] V. Luginbuehl, N. Meier, K. Kovar, J. Rohrer, Intracellular drug delivery: Potential usefulness of engineered Shiga toxin subunit B for targeted cancer therapy, Biotechnol. Adv. 36 (2018) 613–623.

[56] M.K. Manshadi, M. Saadat, M. Mohammadi, M. Shamsi, M. Dejam, R. Kamali, A. Sanati-Nezhad, Delivery of magnetic micro/nanoparticles and magnetic-based drug/cargo into arterial flow for targeted therapy, Drug Deliv. 25 (2018) 1963–1973.

[57] M. Sabz, R. Kamali, S. Ahmadizade, Controlled release of magnetic particles for drug delivery in the human lung, IEEE Trans. Mag. 56 (2020) 1–11.

[58] M.J.J. Shinkai, Functional magnetic particles for medical application, J. Biosci. Bioeng. 94 (2002) 606–613.

[59] M. Johannsen, U. Gneveckow, B. Thiesen, K. Taymoorian, C.H. Cho, N. Waldöfner, R. Scholz, A. Jordan, S.A. Loening, P.J.E.u. Wust, Thermotherapy of prostate cancer using magnetic nanoparticles: Feasibility, imaging, and three-dimensional temperature distribution, Eur. Urol. 52 (2007) 1653–1662.

[60] Z. Saiyed, S. Telang, C. Ramchand, Application of magnetic techniques in the field of drug discovery and biomedicine, BioMag. Res. Technol. 1 (2003) 2.

[61] M. Larimi, A. Ramiar, A. Ranjbar, Numerical simulation of magnetic nanoparticles targeting in a bifurcation vessel, J. Magnet. Mag. Mater. 362 (2014) 58–71.

[62] M. Momeni Larimi, A. Ramiar, A.A. Ranjbar, Magnetic nanoparticles and blood flow behavior in non-Newtonian pulsating flow within the carotid artery in drug delivery application, Proc. Inst. Mech. Eng. Part H J. Eng. Med. 230 (2016) 876–891.

[63] S. Kenjereš, B. Righolt, Simulations of magnetic capturing of drug carriers in the brain vascular system, Int. J. Heat Fluid Flow 35 (2012) 68–75.

[64] M. Shamsi, A. Sedaghatkish, M. Dejam, M. Saghafian, M. Mohammadi, A. Sanati-Nezhad, Magnetically assisted intraperitoneal drug delivery for cancer chemotherapy, Drug Deliv. 25 (2018) 846–861.

[65] J. Patil, S. Sarasija, Pulmonary drug delivery strategies: A concise, systematic review, Lung India Off. Organ Ind. Chest Society 29 (2012) 44.

[66] L.A. Torre, R.L. Siegel, A. Jemal, Lung cancer statistics, Lung cancer and personalized medicine, Springer, 2016, pp. 1–19.

[67] M. Riihimäki, A. Hemminki, M. Fallah, H. Thomsen, K. Sundquist, J. Sundquist, K. Hemminki, Metastatic sites and survival in lung cancer, Lung Cancer 86 (2014) 78–84.

[68] V. Kumar, A.K. Abbas, J.C. Aster, Robbins basic pathology e-book, Elsevier Health Sciences, 2017.

[69] M. Noguchi, Stepwise progression of pulmonary adenocarcinoma—clinical and molecular implications, Cancer Metastasis Rev. 29 (2010) 15–21.

[70] K. Kadota, J. Villena-Vargas, A. Yoshizawa, N. Motoi, C.S. Sima, G.J. Riely, V.W. Rusch, P.S. Adusumilli, W.D. Travis, Prognostic significance of adenocarcinoma in situ, minimally invasive adenocarcinoma, and nonmucinous lepidic predominant invasive adenocarcinoma of the lung in patients with stage I disease, Am. J. Surg. Pathol. 38 (2014) 448.

[71] J.Y. Son, H.Y. Lee, K.S. Lee, J.-H. Kim, J. Han, J.Y. Jeong, O.J. Kwon, Y.M. Shim, Quantitative CT analysis of pulmonary ground-glass opacity nodules for the distinction of invasive adenocarcinoma from pre-invasive or minimally invasive adenocarcinoma, PLoS One 9 (2014) e104066.

[72] K. Funai, T. Yokose, G.-i. Ishii, K. Araki, J. Yoshida, M. Nishimura, K. Nagai, Y. Nishiwaki, A. Ochiai, Clinicopathologic characteristics of peripheral squamous cell carcinoma of the lung, Am. J. Surg. Pathol. 27 (2003) 978–984.

[73] M. Sereno, I.R. Esteban, F. Zambrana, M. Merino, C. Gómez-Raposo, M. López-Gómez, E.C. Sáenz, Squamous-cell carcinoma of the lungs: Is it really so different? Crit. Rev. Oncol. Hematol. 84 (2012) 327–339.

[74] M.K. Santos, T. Muley, A. Warth, W.D. de Paula, M. Lederlin, P.A. Schnabel, H.-P. Schlemmer, H.-U. Kauczor, C.P. Heussel, M. Puderbach, Morphological computed tomography features of surgically resectable pulmonary squamous cell carcinomas: Impact on prognosis and comparison with adenocarcinomas, Eur. J. Radiol. 83 (2014) 1275–1281.

[75] S. Blackmon, A. Ernst, P.T. Cagle, T.C. Allen, D.R. Mody, N.P. Ohori, E.R. Hoff,

[76] A.E. Fraire, Squamous cell carcinoma, Atlas of Neoplastic Pulmonary Disease, Springer, 2010, pp. 139–143.

[76] E. Dulmet-Brender, F. Jaubert, G. Huchon, Exophytic endobronchial epidermoid carcinoma, Cancer 57 (1986) 1358–1364.

[77] A.M. Marchevsky, M.R. Wick, Diagnostic difficulties with the diagnosis of small cell carcinoma of the lung, Seminars in Diagnostic Pathology, Elsevier, 2015, pp. 480–488.

[78] D.K. Das, A.T. Muqim, B.I. Haji, K. Al-Bishi, R. Abdulghani, Pancreatic metastasis in a case of small cell lung carcinoma: Diagnostic role of fine-needle aspiration cytology and immunocytochemistry, J. Cytol./Ind. Acad. Cytol. 28 (2011) 226.

[79] T. Suduł, J. Domagała-Kulawik, Clinical manifestation and radiological features of small cell lung cancer (SCLC), Wiadomosci lekarskie, (Warsaw, Poland: 1960) 65 (2012) 97–101.

[80] S. Khetani, M. Mohammadi, A. Sanati Nezhad, Filter-based isolation, enrichment, and characterization of circulating tumor cells, Biotechnol. Bioeng. 115 (2018) 2504–2529.

[81] M.B. Amin, S.B. Edge, AJCC Cancer Staging Manual, Springer, 2017.

[82] Y.-Q. Chen, Y. Yang, Y.-F. Xing, S. Jiang, X.-W. Sun, Detection of rib metastases in patients with lung cancer: A comparative study of MRI, CT and bone scintigraphy, PLoS One 7 (2012) e52213.

[83] G.A. Silvestri, A.V. Gonzalez, M.A. Jantz, M.L. Margolis, M.K. Gould, L.T. Tanoue, L.J. Harris, F.C. Detterbeck, Methods for staging non-small cell lung cancer: diagnosis and management of lung cancer: American College of Chest Physicians evidence-based clinical practice guidelines, Chest 143 (2013) e211S–e250S.

[84] K.Y. Lam, C.Y. Lo, Metastatic tumours of the adrenal glands: A 30-year experience in a teaching hospital, Clin. Endocrinol. (Oxf) 56 (2002) 95–101.

[85] S. Bovio, A. Cataldi, G. Reimondo, P. Sperone, S. Novello, A. Berruti, P. Borasio, C. Fava, L. Dogliotti, G.V. Scagliotti, Prevalence of adrenal incidentaloma in a contemporary computerized tomography series, J. Endocrinol. Invest. 29 (2006) 298–302.

[86] K. Kagohashi, H. Satoh, H. Ishikawa, M. Ohtsuka, K. Sekizawa, Liver metastasis at the time of initial diagnosis of lung cancer, Med. Oncol. 20 (2003) 25–28.

[87] P.L. Filosso, E. Ruffini, P.O. Lausi, M. Lucchi, A. Oliaro, F. Detterbeck, Historical perspectives: The evolution of the thymic epithelial tumors staging system, Lung Cancer 83 (2014) 126–132.

[88] D. Morgensztern, S. Waqar, J. Subramanian, K. Trinkaus, R. Govindan, Prognostic impact of malignant pleural effusion at presentation in patients with metastatic non-small-cell lung cancer, J. Thorac. Oncol. 7 (2012) 1485–1489.

[89] J.M. Porcel, A. Esquerda, M. Vives, S. Bielsa, Etiology of pleural effusions: Analysis of more than 3,000 consecutive thoracenteses, Arch. Bronconeumol. (Engl. Ed.) 50 (2014) 161–165.

[90] P. Perez-Moreno, E. Brambilla, R. Thomas, J.-C. Soria, Squamous cell carcinoma of the lung: Molecular subtypes and therapeutic opportunities, Clin. Cancer Res. 18 (2012) 2443–2451.

[91] W. Pao, J. Chmielecki, Rational, biologically based treatment of EGFR-mutant non-small-cell lung cancer, Nat. Rev. Cancer 10 (2010) 760.

[92] M. Früh, D. De Ruysscher, S. Popat, L. Crinò, S. Peters, E. Felip, E.G.W. Group, Small-cell lung cancer (SCLC): ESMO Clinical Practice Guidelines for diagnosis, treatment and follow-up, Ann. Oncol. 24 (2013) vi99–vi105.

[93] J.P. van Meerbeeck, D.A. Fennell, D.K. De Ruysscher, Small-cell lung cancer, The Lancet 378 (2011) 1741–1755.

[94] C. Lengauer, K.W. Kinzler, B. Vogelstein, Genetic instabilities in human cancers, Nature 396 (1998) 643.

[95] S. Soleimani, M. Shamsi, M.A. Ghazani, H.P. Modarres, K.P. Valente, M. Saghafian, M.M. Ashani, M. Akbari, A. Sanati-Nezhad, Translational models of tumor angiogenesis: A nexus of in silico and in vitro models, Biotechnol. Adv. 36 (4) (2018) 880–893.

[96] K.M. Fong, Y. Sekido, J.D. Minna, Molecular pathogenesis of lung cancer, J. Thorac. Cardiovasc. Surg. 118 (1999) 1136–1152.

[97] T. Kawaguchi, Y. Koh, M. Ando, N. Ito, S. Takeo, H. Adachi, T. Tagawa, S. Kakegawa, M. Yamashita, K. Kataoka, Prospective analysis of oncogenic driver mutations and environmental factors: Japan Molecular Epidemiology for Lung Cancer Study, J. Clin. Oncol. 34 (2016) 2247–2257.

[98] V.L. Keedy, S. Temin, M.R. Somerfield, M.B. Beasley, D.H. Johnson, L.M. McShane, D.T. Milton, J.R. Strawn, H.A. Wakelee, G. Giaccone, American Society of Clinical Oncology provisional clinical opinion: epidermal growth factor receptor (EGFR) mutation testing for patients with advanced non–small-cell lung cancer considering first-line EGFR tyrosine kinase inhibitor therapy, J. Clin. Oncol. 29 (2011) 2121–2127.

[99] S.P. D'Angelo, M.C. Pietanza, The molecular pathogenesis of small cell lung cancer, Cancer Biol. Ther. 10 (2010) 1–10.

[100] K.J. O'Byrne, U. Gatzemeier, I. Bondarenko, C. Barrios, C. Eschbach, U.M. Martens, Y. Hotko, C. Kortsik, L. Paz-Ares, J.R. Pereira, Molecular biomarkers in non-small-cell lung cancer: A retrospective analysis of data from the phase 3 FLEX study, Lancet Oncol. 12 (2011) 795–805.

[101] J.H. Paik, G. Choe, H. Kim, J.Y. Choe, H.J. Lee, C.T. Lee, J.S. Lee, J. Sheon, J.-H. Chung, Screening of anaplastic lymphoma kinase rearrangement by immunohistochemistry in non-small cell lung cancer: Correlation with fluorescence in situ hybridization, J. Thorac. Oncol. 6 (2011) 466–472.

[102] V.M. Rimkunas, K.E. Crosby, D. Li, Y. Hu, M.E. Kelly, T.-L. Gu, J.S. Mack, M.R. Silver, X. Zhou, H. Haack, Analysis of receptor tyrosine kinase ROS1-positive tumors in non–small cell lung cancer: Identification of a FIG-ROS1 fusion, Clin. Cancer Res. 18 (2011) 4449–4457.

[103] A. Yoshida, K. Tsuta, S. Wakai, Y. Arai, H. Asamura, T. Shibata, K. Furuta, T. Kohno, R. Kushima, Immunohistochemical detection of ROS1 is useful for identifying ROS1 rearrangements in lung cancers, Mod. Pathol. 27 (2014) 711.

[104] T. Kinno, K. Tsuta, K. Shiraishi, T. Mizukami, M. Suzuki, A. Yoshida, K. Suzuki, H. Asamura, K. Furuta, T. Kohno, Clinicopathological features of nonsmall cell lung carcinomas with BRAF mutations, Ann. Oncol. 25 (2013) 138–142.

[105] T. Li, H.-J. Kung, P.C. Mack, D.R. Gandara, Genotyping and genomic profiling of non-small-cell lung cancer: Implications for current and future therapies, J. Clin. Oncol. 31 (2013) 1039.

[106] A.F. Farago, L.P. Le, Z. Zheng, A. Muzikansky, A. Drilon, M. Patel, T.M. Bauer, S.V. Liu, S.-H.I. Ou, D. Jackman, Durable clinical response to entrectinib in NTRK1-rearranged non-small cell lung cancer, J. Thorac. Oncol. 10 (2015) 1670–1674.

[107] M.E. Arcila, J.E. Chaft, K. Nafa, S. Roy-Chowdhuri, C. Lau, M. Zaidinski, P.K. Paik, M.F. Zakowski, M.G. Kris, M. Ladanyi, Prevalence, clinicopathologic associations, and molecular spectrum of ERBB2 (HER2) tyrosine kinase mutations in lung adenocarcinomas, Clin. Cancer Res. 18 (2012) 4910–4918.

[108] D.M. Hickinson, T. Klinowska, G. Speake, J. Vincent, C. Trigwell, J. Anderton, S. Beck, G. Marshall, S. Davenport, R. Callis, AZD8931, an equipotent, reversible inhibitor of signaling by epidermal growth factor receptor, ERBB2 (HER2), and ERBB3: A unique agent for simultaneous ERBB receptor blockade in cancer, Clin. Cancer Res. 16 (2010) 1159–1169.

[109] P.C. Ma, T. Kijima, G. Maulik, E.A. Fox, M. Sattler, J.D. Griffin, B.E. Johnson, R. Salgia, c-MET mutational analysis in small cell lung cancer: Novel juxtamembrane domain mutations regulating cytoskeletal functions, Cancer Res. 63 (2003) 6272–6281.

[110] T. Kubo, H. Yamamoto, W.W. Lockwood, I. Valencia, J. Soh, M. Peyton, M. Jida, H. Otani, T. Fujii, M. Ouchida, MET gene amplification or EGFR mutation activate MET in lung cancers untreated with EGFR tyrosine kinase inhibitors, Int. J. Cancer 124 (2009) 1778–1784.

[111] K. Okuda, H. Sasaki, H. Yukiue, M. Yano, Y. Fujii, Met gene copy number predicts the prognosis for completely resected non-small cell lung cancer, Cancer Sci. 99 (2008) 2280–2285.

[112] X. Liu, Y. Jia, M.B. Stoopler, Y. Shen, H. Cheng, J. Chen, M. Mansukhani, S. Koul, B. Halmos, A.C. Borczuk, Next-generation sequencing of pulmonary sarcomatoid carcinoma reveals high frequency of actionable MET gene mutations, J. Clin. Oncol. 34 (2016) 794–802.

[113] M. Esteller, M. Sanchez-Cespedes, R. Rosell, D. Sidransky, S.B. Baylin, J.G. Herman, Detection of aberrant promoter hypermethylation of tumor suppressor genes in serum DNA from non-small cell lung cancer patients, Cancer Res. 59 (1999) 67–70.

[114] T. Jacks, A. Fazeli, E.M. Schmitt, R.T. Bronson, M.A. Goodell, R.A. Weinberg, Effects of an Rb mutation in the mouse, Nature 359 (1992) 295.

[115] G. Jin, M.J. Kim, H.-S. Jeon, J.E. Choi, D.S. Kim, E.B. Lee, S.I. Cha, G.S. Yoon, C.H. Kim, T.H. Jung, PTEN mutations and relationship to EGFR, ERBB2, KRAS, and TP53 mutations in non-small cell lung cancers, Lung Cancer 69 (2010) 279–283.

[116] H. Wang, L. Zheng, C. Peng, M. Shen, X. Shi, G. Zhang, Folic acid-modified dendrimer-entrapped gold nanoparticles as nanoprobes for targeted CT imaging of human lung adencarcinoma, Biomaterials 34 (2013) 470–480.

[117] V. Francisco, M. Koenigkam-Santos, D.T. Wada, J.R.F. Junior, A.T. Fabro, F.E.G. Cipriano, S.G. Quatrina, P.M. de Azevedo-Marques, Computer-aided diagnosis of lung cancer in magnetic resonance imaging exams, XXVI Brazilian Congress on Biomedical Engineering, Springer, 2019, pp. 121–127.

[118] J.D. Predina, A.D. Newton, C. Corbett, M. Shin, L.F. Sulfyok, O.T. Okusanya, E.J. Delikatny, S. Nie, C. Gaughan, D. Jarrar, Near-infrared intraoperative imaging for minimally invasive pulmonary metastasectomy for sarcomas, J. Thorac. Cardiovasc. Surg. 157 (2019) 2061–2069.

[119] S.A. Nehmeh, Y.E. Erdi, Respiratory motion in positron emission tomography/computed tomography: A review, Seminars in Nuclear Medicine, Elsevier, 2008, pp. 167–176.

[120] A.T. Fernandes, J. Shen, J. Finlay, N. Mitra, T. Evans, J. Stevenson, C. Langer, L. Lin, S. Hahn, E. Glatstein, Elective nodal irradiation (ENI) vs. involved field radiotherapy (IFRT) for locally advanced non-small-cell lung cancer (NSCLC): A comparative analysis of toxicities and clinical outcomes, Radiother. Oncol. 95 (2010) 178–184.

[121] J.R. Jett, Limitations of screening for lung cancer with low-dose spiral computed tomography, Clin. Cancer Res. 11 (2005) 4988s–4992s.

[122] P.B. Bach, J.N. Mirkin, T.K. Oliver, C.G. Azzoli, D.A. Berry, O.W. Brawley, T. Byers, G.A. Colditz, M.K. Gould, J.R. Jett, Benefits and harms of CT screening for lung cancer: A systematic review, JAMA 307 (2012) 2418–2429.

[123] A. Billé, E. Pelosi, A. Skanjeti, V. Arena, L. Errico, P. Borasio, M. Mancini, F. Ardissone, Preoperative intrathoracic lymph node staging in patients with non-small-cell lung cancer: Accuracy of integrated positron emission tomography and computed tomography, Eur. J. Cardiothorac. Surg. 36 (2009) 440–445.

[124] T.P. Brea, A.R. Raviña, A.G. Gómez, A.M. de Alegría, L. Valdèc, Use of magnetic resonance imaging for N-staging in patients with non-small cell lung cancer. A systematic review, Arch. Bronconeumol. (Engl. Ed.) 55 (2019) 9–16.

[125] S. Laurent, D. Forge, M. Port, A. Roch, C. Robic, L. Vander Elst, R.N.J.C.r. Muller, Magnetic iron oxide nanoparticles: Synthesis, stabilization, vectorization, physicochemical characterizations, and biological applications, Chem. Rev. 108 (2008) 2064–2110.

[126] J. Yang, Y. Luo, Y. Xu, J. Li, Z. Zhang, H. Wang, M. Shen, X. Shi, G. Zhang, Conjugation of iron oxide nanoparticles with RGD-modified dendrimers for targeted tumor MR imaging, ACS Appl. Mater. Interfaces 7 (2015) 5420–5428.

[127] K.E. Albinali, M.M. Zagho, Y. Deng, A.A. Elzatahry, A perspective on magnetic core–shell carriers for responsive and targeted drug delivery systems, Int. J. Nanomedicine 14 (2019) 1707.

[128] C. Chen, H. Yu, R. Xia, L. Wang, S. Liu, Z. Xu, X. Xiao, F. Gao, Magnetic

[129] resonance tracking of endothelial progenitor cells labeled with alkyl-polyethylenimine 2 kDa/superparamagnetic iron oxide in a mouse lung carcinoma xenograft model, Mol. Imaging 13 (2014) 7290.2014.00030.

[129] M.-K. Yoo, I.-K. Park, H.-T. Lim, S.-J. Lee, H.-L. Jiang, Y.-K. Kim, Y.-J. Choi, M.-H. Cho, C.-S. Cho, Folate–PEG–superparamagnetic iron oxide nanoparticles for lung cancer imaging, Acta Biomater. 8 (2012) 3005–3013.

[130] X. Hao, B. Xu, H. Chen, X. Wang, J. Zhang, R. Guo, X. Shi, X. Cao, Stem cell-mediated delivery of nanogels loaded with ultrasmall iron oxide nanoparticles for enhanced tumor MR imaging, Nanoscale 11 (2019) 4904–4910.

[131] L. Yan, L. Luo, A. Amirshaghaghi, J. Miller, C. Meng, T. You, T.M. Busch, A. Tsourkas, Z. Cheng, Dextran-Benzoporphyrin derivative (BPD) coated superparamagnetic iron oxide nanoparticle (SPION) micelles for T2-weighted magnetic resonance imaging and photodynamic therapy, Bioconjug. Chem. 30 (2019) 2974–2981.

[132] J.S. Guthi, S.-G. Yang, G. Huang, S. Li, C. Khemtong, C.W. Kessinger, M. Peyton, J.D. Minna, K.C. Brown, J.J.M.p. Gao, MRI-visible micellar nanomedicine for targeted drug delivery to lung cancer, Cells 7 (2009) 32–40.

[133] C. Medina, M. Santos-Martinez, A. Radomski, O. Corrigan, M. Radomski, Nanoparticles: Pharmacological and toxicological significance, Br. J. Pharmacol. 150 (2007) 552–558.

[134] A.K. Gupta, M. Gupta, Synthesis and surface engineering of iron oxide nanoparticles for biomedical applications, Biomaterials 26 (2005) 3995–4021.

[135] V.I. Shubayev, T.R. Pisanic II, S. Jin, Magnetic nanoparticles for theragnostics, Adv. Drug Deliv. Rev. 61 (2009) 467–477.

[136] H. Koyama, Y. Ohno, S. Seki, M. Nishio, T. Yoshikawa, S. Matsumoto, K. Sugimura, Magnetic resonance imaging for lung cancer, J. Thoracic Dis. 28 (2013) 138–150.

[137] Q. Chang, N. Wu, H. Ouyang, Y.J.C.i. Huang, Diffusion-weighted magnetic resonance imaging of lung cancer at 3.0 T: A preliminary study on monitoring diffusion changes during chemoradiation therapy, Clin. Imaging 36 (2012) 98–103.

[138] K. Usuda, A. Funasaki, A. Sekimura, N. Motono, M. Matoba, M. Doai, S. Yamada, Y. Ueda, H. Uramoto, FDG-PET/CT and diffusion-weighted imaging for resected lung cancer: Correlation of maximum standardized uptake value and apparent diffusion coefficient value with prognostic factors, Med. Oncol. 35 (2018) 66.

[139] S.H. Yoon, J.M. Goo, S.M. Lee, C.M. Park, H.J. Seo, G.J. Cheon, Positron emission tomography/magnetic resonance imaging evaluation of lung cancer: Current status and future prospects, J. Thoracic Imaging 29 (2014) 4–16.

[140] T.S. Wiedmann, A. Ravichandran, Ultrasonic nebulization system for respiratory drug delivery, Pharm. Dev.Technol. 6 (2001) 83–89.

[141] A. Papachristodoulou, R.D. Signorell, B. Werner, D. Brambilla, P. Luciani, M. Cavusoglu, J. Grandjean, M. Silginer, M. Rudin, E. Martin, Chemotherapy sensitization of glioblastoma by focused ultrasound-mediated delivery of therapeutic liposomes, J. Control. Release 295 (2019) 130–139.

[142] M. Meier-Schroers, R. Homsi, D. Skowasch, J. Buermann, M. Zipfel, H.H. Schild, D.J. Thomas, Lung cancer screening with MRI: Results of the first screening round, Eur. Radiol. 144 (2018) 117–125.

[143] A. Cieszanowski, A. Lisowska, M. Dabrowska, P. Korczynski, M. Zukowska, I.P. Grudzinski, R. Pacho, O. Rowinski, R. Krenke, MR imaging of pulmonary nodules: Detection rate and accuracy of size estimation in comparison to computed tomography, PLoS One 11 (2016) e0156272.

[144] H. Nomori, T. Mori, K. Ikeda, K. Kawanaka, S. Shiraishi, K. Katahira, Y. Yamashita, Diffusion-weighted magnetic resonance imaging can be used in place of positron emission tomography for N staging of non-small cell lung cancer with fewer false-positive results, J. Thorac. Cardiovasc. Surg. 135 (2008) 816–822.

[145] K. Usuda, S. Maeda, N. Motono, M. Ueno, M. Tanaka, Y. Machida, M. Matoba, N. Watanabe, H. Tonami, Diagnostic performance of diffusion-weighted imaging for multiple hilar and mediastinal lymph nodes with FDG accumulation, Asian Pac. J. Cancer Prev. 16 (2015) 6401–6406.

[146] K. Krupa, M.J. Bekiesińska-Figatowska, Artifacts in magnetic resonance imaging, Pol. J. Radiol. 80 (2015) 93.

[147] J. Kirchner, C. Deuschl, J. Grueneisen, K. Herrmann, M. Forsting, P. Heusch, G. Antoch, L. Umutlu, 18 F-FDG PET/MRI in patients suffering from lymphoma: How much MRI information is really needed? Eur. J. Nuclear Med. Mol. Imaging 44 (2017) 1005–1013.

[148] A.C. Sher, V. Seghers, M.J. Paldino, C. Dodge, R. Krishnamurthy, R. Krishnamurthy, E.M. Rohren, Assessment of sequential PET/MRI in comparison with PET/CT of pediatric lymphoma: A prospective study, Am. J. Roentgenol. 206 (2016) 623–631.

[149] F. Nensa, K. Beiderwellen, P. Heusch, A. Wetter, Clinical applications of PET/MRI: Current status and future perspectives, Diagn. Interv. Radiol. 20 (2014) 438.

[150] K. Usuda, A. Funazaki, R. Maeda, A. Sekimura, N. Motono, M. Matoba, Economic benefits and diagnostic quality of diffusion-weighted magnetic resonance imaging for primary lung cancer, Ann. Thorac. Cardiovasc. Surg. (2017) 17–00097.

[151] R.a. Weissleder, D.D. Stark, B.L. Engelstad, B.R. Bacon, C.C. Compton, D.L. White, P. Jacobs, J. Lewis, Superparamagnetic iron oxide: Pharmacokinetics and toxicity, Am. J. Roentgenol. 152 (1989) 167–173.

[152] V. Orel, A. Shevchenko, A. Romanov, M. Tselepi, T. Mitrelias, C.H. Barnes, A. Burlaka, S. Lukin, I. Shchepotin, Magnetic properties and antitumor effect of nanocomplexes of iron oxide and doxorubicin, Nanomed. Nanotechnol. Biol. Med. 11 (2015) 47–55.

[153] L. Sadeghi, H. Espanani, Toxic effects of the Fe2O3 nanoparticles on the liver and lung tissue, Bratisl. Lek. Listy 116 (2015) 373–378.

[154] Y. Yang, Q. Guo, J. Peng, J. Su, X. Lu, Y. Zhao, Z. Qian, Doxorubicin-conjugated heparin-coated superparamagnetic iron oxide nanoparticles for combined anticancer drug delivery and magnetic resonance imaging, J. Biomed. Nanotechnol. 12 (2016) 1963–1974.

[155] D.L. Huber, Synthesis, properties, and applications of iron nanoparticles, Small 1

(2005) 482–501.

[156] P. De La Presa, M. Multigner, M. Morales, T. Rueda, E. Fernandez-Pinel, A. Hernando, Synthesis and characterization of FePt/Au core-shell nanoparticles, J. Magnet. Mag. Mater. 316 (2007) e753–e755.

[157] L.B. Laurentius, N.A. Owens, J. Park, A.C. Crawford, M.D. Porter, Advantages and limitations of nanoparticle labeling for early diagnosis of infection, Expert Rev. Mol. Diagn. 16 (2016) 883–895.

[158] J. Kudr, Y. Haddad, L. Richtera, Z. Heger, M. Cernak, V. Adam, O. Zitka, Magnetic nanoparticles: From design and synthesis to real world applications, Nanomaterials 7 (2017) 243.

[159] T. Li, G. Yan, Y. Bai, M. Wu, G. Fang, M. Zhang, Y. Xie, A. Borjigidai, B. Fu, Papain bioinspired gold nanoparticles augmented the anticancer potency of 5-FU against lung cancer, J. Exp. Nanosci. 15 (2020) 109–128.

[160] M. Rozalen, M. Sánchez-Polo, M. Fernández-Perales, T. Widmann, J. Rivera-Utrilla, Synthesis of controlled-size silver nanoparticles for the administration of methotrexate drug and its activity in colon and lung cancer cells, RSC Adv. 10 (2020) 10646–10660.

[161] C.-L. Tseng, K.-C. Chang, M.-C. Yeh, K.-C. Yang, T.-P. Tang, F.-H. Lin, Development of a dual-functional Pt–Fe-HAP magnetic nanoparticles application for chemo-hyperthermia treatment of cancer, Ceram. Int. 40 (2014) 5117–5127.

[162] S. Sun, Recent advances in chemical synthesis, self-assembly, and applications of FePt nanoparticles, Adv. Mater. 18 (2006) 393–403.

[163] A.H. Faraji, P. Wipf, Nanoparticles in cellular drug delivery, Bioorg. Med. Chem. 17 (2009) 2950–2962.

[164] R. Singh, J.W. Lillard Jr., Nanoparticle-based targeted drug delivery, Exp. Mol. Pathol. 86 (2009) 215–223.

[165] K. Nejati-Koshki, M. Mesgari, E. Ebrahimi, F. Abbasalizadeh, S. Fekri Aval, A.A. Khandaghi, M. Abasi, A. Akbarzadeh, Synthesis and in vitro study of cisplatin-loaded Fe3O4 nanoparticles modified with PLGA-PEG6000 copolymers in treatment of lung cancer, J. Microencapsul. 31 (2014) 815–823.

[166] A. Kumar, P.K. Jena, S. Behera, R.F. Lockey, S. Mohapatra, S. Mohapatra, Multifunctional magnetic nanoparticles for targeted delivery, Nanomed. Nanotechnol. Biol. Med. 6 (2010) 64–69.

[167] N.K. Verma, K. Crosbie-Staunton, A. Satti, S. Gallagher, K.B. Ryan, T. Doody, C. McAtamney, R. MacLoughlin, P. Galvin, C.S. Burke, Magnetic core-shell nanoparticles for drug delivery by nebulization, J. Nanobiotechnol. 11 (2013) 1.

[168] S. Amirsaadat, Y. Pilehvar-Soltanahmadi, F. Zarghami, S. Alipour, Z. Ebrahimnezhad, N. Zarghami, Silibinin-loaded magnetic nanoparticles inhibit hTERT gene expression and proliferation of lung cancer cells, Artificial Cells, Nanomed. Biotechnol. 45 (2017) 1649–1656.

[169] M. Farshbaf, R. Salehi, N. Annabi, R. Khalilov, A. Akbarzadeh, S. Davaran, pH-and thermo-sensitive MTX-loaded magnetic nanocomposites: Synthesis, characterization, and in vitro studies on A549 lung cancer cell and MR imaging, Drug Dev. Ind. Pharm. 44 (2018) 452–462.

[170] M.O. Avilés, A.D. Ebner, J.A. Ritter, In vitro study of magnetic particle seeding for implant assisted-magnetic drug targeting, J. Magnet. Mag. Mater. 320 (2008) 2640–2646.

[171] L. Xu, M.-J. Kim, K.-D. Kim, Y.-H. Choa, H.-T. Kim, Surface modified Fe3O4 nanoparticles as a protein delivery vehicle, Colloids Surf. A Physicochem. Eng. Asp. 350 (2009) 8–12.

[172] B. Chertok, A.E. David, B.A. Moffat, V.C. Yang, Substantiating in vivo magnetic brain tumor targeting of cationic iron oxide nanocarriers via adsorptive surface masking, Biomaterials 30 (2009) 6780–6787.

[173] M. Moravej, M. Mantovani, Biodegradable metals for cardiovascular stent application: Interests and new opportunities, Int. J. Mol. Sci. 12 (2011) 4250–4270.

[174] H.G. Colt Dumon, Tracheobronchial stents: Indications and applications, Lung Cancer 9 (1993) 301–306.

[175] T. Lammers, P. Koczera, S. Fokong, F. Gremse, J. Ehling, M. Vogt, A. Pich, G. Storm, M. Van Zandvoort, Theranostic uspio-loaded microbubbles for mediating and monitoring blood-brain barrier permeation, Adv. Funct. Mater. 25 (2015) 36–43.

[176] S. Wang, Y. Zhou, J. Tan, J. Xu, J. Yang, Y. Liu, Computational modeling of magnetic nanoparticle targeting to stent surface under high gradient field, Computat. Mech. 53 (2014) 403–412.

[177] C. Alexiou, R.J. Schmid, R. Jurgons, M. Kremer, G. Wanner, C. Bergemann, E. Huenges, T. Nawroth, W. Arnold, F.G. Parak, Targeting cancer cells: Magnetic nanoparticles as drug carriers, Eur. Biophys. J. 35 (2006) 446–450.

[178] C. Alexiou, A. Schmidt, R. Klein, P. Hulin, C. Bergemann, W. Arnold, Magnetic drug targeting: Biodistribution and dependency on magnetic field strength, J. Magnet. Mag. Mater. 252 (2002) 363–366.

[179] O. Mykhaylyk, N. Dudchenko, A. Dudchenko, Materials, doxorubicin magnetic conjugate targeting upon intravenous injection into mice: High gradient magnetic field inhibits the clearance of nanoparticles from the blood, J. Magnet. Mag. Mater. 293 (2005) 473–482.

[180] T. Yu, M.-Y. Hua, J.-p. Chen, K.-C. Wei, S.-M. Jung, Y.-J. Chang, M.J. Jou, Effects of external magnetic field on biodistribution of nanoparticles: A histological study, J. Magnet. Mag. Mater. 311 (2007) 372–375.

[181] N.S. Elbialy, M.M. Fathy, W.M. Khalil, Doxorubicin loaded magnetic gold nanoparticles for in vivo targeted drug delivery, J. Magnet. Mag. Mater. 490 (2015) 190–199.

[182] D. Vlaskou, O. Mykhaylyk, F. Krötz, N. Hellwig, R. Renner, U. Schillinger, B. Gleich, A. Heidsieck, G. Schmitz, K. Hensel, Magnetic and acoustically active lipospheres for magnetically targeted nucleic acid delivery, Adv. Funct. Mater. 20 (2010) 3881–3894.

[183] Y. Jia, M. Yuan, H. Yuan, X. Huang, X. Sui, X. Cui, F. Tang, J. Peng, J. Chen, S. Lu, Co-encapsulation of magnetic Fe3O4 nanoparticles and doxorubicin into biodegradable PLGA nanocarriers for intratumoral drug delivery, J. Magnet. Mag. Mater. 7 (2012) 1697.

[184] Guidelines on limits of exposure to static magnetic fields, Health Physics, 96 (2009), pp. 504–514.

[185] M.O. Avilés, A.D. Ebner, M. Ritter, In vitro study of magnetic particle seeding for implant-assisted-magnetic drug targeting: Seed and magnetic drug carrier particle capture, J. Magnet. Mag. Mater. 321 (2009) 1586–1590.

[186] S. Nishijima, F. Mishima, T. Terada, S. Takeda, A study on magnetically targeted drug delivery system using superconducting magnet, Phys. C Superconduct. Appl. 463 (2007) 1311–1314.

[187] M. Chuzawa, F. Mishima, Y. Akiyama, S. Nishijima, Drug accumulation by means of noninvasive magnetic drug delivery system, Front. Chem. 471 (2011) 1538–1542.

[188] Z. Zhang, C. Kleinstreuer, Airflow structures and nano-particle deposition in a human upper airway model, J. Comput. Phys. 198 (2004) 178–210.

[189] F. Russo, A. Boghi, F. Gori, Numerical simulation of magnetic nano drug targeting in patient-specific lower respiratory tract, J. Magnet. Mag. Mater. 451 (2018) 554–564.

[190] E.M. Cherry, P.G. Maxim, J. Eaton, Particle size, magnetic field, and blood velocity effects on particle retention in magnetic drug targeting, Med. Phys. 37 (2010) 175–182.

[191] W. Tao, M. Zhang, A genetic algorithm–based area coverage approach for controlled drug delivery using microrobots, Nanomed. Nanotechnol. Biol. Med. 1 (2005) 91–100.

[192] N. Kumar, S. Hassan, J. Yoon, Optimized targeting of magnetic nano particles for drug delivery system, 2013 IEEE/ASME International Conference on Advanced Intelligent Mechatronics, IEEE, 2013, pp. 585–590.

[193] A. Heidsieck, S. Vosen, K. Zimmermann, D. Wenzel, B. Gleich, Analysis of trajectories for targeting of magnetic nanoparticles in blood vessels, Mol. Pharm. 9 (2012) 2029–2038.

[194] S. Kenjereš, Numerical analysis of blood flow in realistic arteries subjected to strong non-uniform magnetic fields, Fluid Flow 29 (2008) 752–764.

[195] I. Rukshin, J. Mohrenweiser, P. Yue, S. Afkhami, Modeling superparamagnetic particles in blood flow for applications in magnetic drug targeting, Fluids 2 (2017) 29.

[196] B. Shapiro, S. Kulkarni, A. Nacev, S. Muro, P.Y. Stepanov, I. Weinberg, Open challenges in magnetic drug targeting, Wires Nanomed. Nanobiotechnol. 7 (2015) 446–457.

[197] L. Agiotis, I. Theodorakos, S. Samothrakitis, S. Papazoglou, I. Zergioti, M. Raptis, Magnetic manipulation of superparamagnetic nanoparticles in a microfluidic system for drug delivery applications, J. Magnet. Magn. Mater. 401 (2016) 956–964.

[198] A. Sarwar, A. Nemirovski, M. Shapiro, Optimal Halbach permanent magnet designs for maximally pulling and pushing nanoparticles, J. Magnet. Magn. Mater. 324 (2012) 742–754.

[199] J.-S. Choi, M. Yoo, Design of Halbach magnet array based on optimization techniques, IEEE Trans. Magnet. 44 (2008) 2361–2366.

[200] L.C. Barnsley, D. Carugo, J. Owen, E.J.P.i.M. Stride, Halbach arrays consisting of cubic elements optimised for high field gradients in magnetic drug targeting applications, Biology 60 (2015) 8303.

[201] K. Halbach, Design of permanent multipole magnets with oriented rare earth cobalt material, Nuclear Instrum. Methods 169 (1980) 1–10.

[202] L.C. Berselli, P. Miloro, A. Menciassi, E. Sinibaldi, Exact solution to the inverse Womersley problem for pulsatile flows in cylindrical vessels, with application to magnetic particle targeting, Appl. Math. Compet. 219 (2013) 5717–5729.

[203] V. Iacovacci, L. Ricotti, E. Sinibaldi, G. Signore, F. Vistoli, A. Menciassi, An intravascular magnetic catheter enables the retrieval of nanoagents from the bloodstream, Adv. Sci. 5 (2018) 1800807.

[204] A. Patronis, R.A. Richardson, S. Schmieschek, B.J. Wylie, R.W. Nash, P. Coveney, Modelling patient-specific magnetic drug targeting within the intracranial vasculature, Front. Physiol. 9 (2018) 331.

[205] M. Sabz, R. Kamali, S. Ahmadizade, Numerical simulation of magnetic drug targeting to a tumor in the simplified model of the human lung, Comput. Methods Programs Biomed. 172 (2019) 11–24.

[206] A.K. Hauser, R.J. Wydra, N.A. Stocke, K.W. Anderson, J.Z. Hilt, Magnetic nanoparticles and nanocomposites for remote controlled therapies, J. Control. Release 219 (2015) 76–94.

[207] H. Wang, L. Wu, X. Sun, Intratracheal delivery of nano-and microparticles and hyperpolarized gases: A promising strategy for imaging and treatment of respiratory disease, Chest 157 (6) (June 2020) 1579–1590.

[208] R. Gradl, M. Dierolf, L. Yang, L. Hehn, B. Günther, W. Möller, D. Kutschke, T. Stoeger, B. Gleich, K. Achterhold, Visualizing treatment delivery and deposition in mouse lungs using in vivo x-ray imaging, J. Control. Release 307 (2019) 282–291.

[209] Y. Ju, C. Cortez-Jugo, J. Chen, T.Y. Wang, A.J. Mitchell, E. Tsantikos, N. Bertleff-Zieschang, Y.W. Lin, J. Song, Y. Cheng, Engineering of nebulized metal–phenolic capsules for controlled pulmonary deposition, Adv. Sci. 1902650 (2020).

[210] A. Rauf, A. Bhatnagar, S. Sisodia, R.K. Khar, F.J. Ahmad, Lungs deposition and pharmacokinetic study of submicron budesonide particles in Wistar rats intended for immediate effect in asthma, EXCLI J. 16 (2017) 236.

[211] P. Dames, B. Gleich, A. Flemmer, K. Hajek, N. Seidl, F. Wiekhorst, D. Eberbeck, I. Bittmann, C. Bergemann, T. Weyh, Targeted delivery of magnetic aerosol droplets to the lung, Nat. Nanotechnol. 2 (2007) 495.

[212] T. Sadhukha, T.S. Wiedmann, J. Panyam, Inhalable magnetic nanoparticles for targeted hyperthermia in lung cancer therapy, Biomaterials 34 (2013) 5163–5171.

[213] D.N. Price, L.R. Stromberg, N.K. Kunda, P. Muttil, In vivo pulmonary delivery and

magnetic-targeting of dry powder nano-in-microparticles, Mol. Pharm. 14 (2017) 4741–4750.

[214] N.K. Verma, K. Crosbie-Staunton, A. Satti, S. Gallagher, K.B. Ryan, T. Doody, C. McAtamney, R. MacLoughlin, P. Galvin, C. Burke, Magnetic core-shell nanoparticles for drug delivery by nebulization, J. Nanobiotechnol. 11 (2013) 1.

[215] G. Hasenpusch, J. Geiger, K. Wagner, O. Mykhaylyk, F. Wiekhorst, L. Trahms, A. Heidsieck, B. Gleich, C. Bergemann, M. Aneja, Magnetized aerosols comprising superparamagnetic iron oxide nanoparticles improve targeted drug and gene delivery to the lung, Pharm. Res. 29 (2012) 1308–1318.

[216] C. Dahmani, S. Gotz, T. Weyh, R. Renner, M. Rosenecker, C. Rudolph, Respiration triggered magnetic drug targeting in the lungs, 2009 Annual International Conference of the IEEE Engineering in Medicine and Biology Society, IEEE, 2009, pp. 5440–5443.

[217] Y. Xie, P.W. Longest, Y.H. Xu, J.P. Wang, T. Wiedmann, In vitro and in vivo lung deposition of coated magnetic aerosol particles, J. Pharm. Sci. 99 (2010) 4658–4668.

[218] J. Ally, B. Martin, M.B. Khamesee, W. Roa, A. Amirfazli, Magnetic targeting of aerosol particles for cancer therapy, J. Magnet. Mag. Mater. 293 (2005) 442–449.

[219] A.R. Martin, W.H. Finlay, Enhanced deposition of high aspect ratio aerosols in small airway bifurcations using magnetic field alignment, J. Aerosol Sci. 39 (2008) 679–690.

[220] Y. Xie, P. Zeng, R.A. Siegel, T.S. Wiedmann, B.E. Hammer, Magnetic deposition of aerosols composed of aggregated superparamagnetic nanoparticles, Pharm. Res. 27 (2010) 855–865.

[221] D. Upadhyay, S. Scalia, R. Vogel, N. Wheate, R.O. Salama, P.M. Young, D. Traini, W. Chrzanowski, Magnetised thermo responsive lipid vehicles for targeted and controlled lung drug delivery, Pharm. Res. 29 (2012) 2456–2467.

[222] F. Tewes, C. Ehrhardt, P. Healy, Superparamagnetic iron oxide nanoparticles (SPIONs)-loaded Trojan microparticles for targeted aerosol delivery to the lung, Eur. J. Pharm. Biopharm. 86 (2014) 98–104.

[223] N.A. Stocke, S.A. Meenach, S.M. Arnold, H.M. Mansour, J. Hilt, Formulation and characterization of inhalable magnetic nanocomposite microparticles (MnMs) for targeted pulmonary delivery via spray drying, Int. J. Pharm. 479 (2015) 320–328.

[224] R. Martinez, A. Roshchenko, P. Minev, W. Finlay, Simulation of enhanced deposition due to magnetic field alignment of ellipsoidal particles in a lung bifurcation, J. Aerosol. Med. Pulm. Drug Deliv. 26 (2013) 31–40.

[225] O. Pourmehran, M. Rahimi-Gorji, M. Gorji-Bandpy, T. Gorji, Simulation of magnetic drug targeting through tracheobronchial airways in the presence of an external non-uniform magnetic field using Lagrangian magnetic particle tracking, J. Magnet. Mag. Mater. 393 (2015) 380–393.

[226] O. Pourmehran, T.B. Gorji, M. Gorji-Bandpy, Magnetic drug targeting through a realistic model of human tracheobronchial airways using computational fluid and particle dynamics, Biomech. Model. Mechanobiol. 15 (2016) 1355–1374.

[227] A. Krafcik, P. Babinec, M. Frollo, Computational analysis of magnetic field induced deposition of magnetic particles in lung alveolus in comparison to deposition produced with viscous drag and gravitational force, J. Magnet. Mag. Mater. 380 (2015) 46–53.

[228] Y. Ostrovski, P. Hofemeier, A. Sznitman, Augmenting regional and targeted delivery in the pulmonary acinus using magnetic particles, Int. J. Nanomedicine 11 (2016) 3385.

[229] S. Kenjereš, R. Tjin, Numerical simulations of targeted delivery of magnetic drug aerosols in the human upper and central respiratory system: A validation study, R. Soc. Open Sci. 4 (2017) 170873.

[230] F. Russo, A. Boghi, M. Gori, Numerical simulation of magnetic nano drug targeting in patient-specific lower respiratory tract, J. Magnet. Mag. Mater. 451 (2018) 554–564.

[231] M. Mohammadian, O. Pourmehran, CFPD simulation of magnetic drug delivery to a human lung using an SAW nebulizer, Biomech. Model. Mechanobiol. 18 (2019) 547–562.

[232] H. Nikookar, O. Abouali, M. Eghtesad, S. Sadrizadeh, S. Ahmadi, Enhancing drug delivery to human trachea through oral airway using magnetophoretic steering of microsphere carriers composed of aggregated superparamagnetic nanoparticles and nanomedicine: A numerical study, J. Aerosol Sci. 127 (2019) 63–92.

[233] M.K. Manshadi, M. Saadat, M. Mohammadi, R. Kamali, M. Shamsi, M. Naseh, A. Sanati-Nezhad, Magnetic aerosol drug targeting in lung cancer therapy using permanent magnet, Drug Deliv. 26 (2019) 120–128.

[234] G.X. Chen, M.H. Wang, T. Zheng, G.C. Tang, F.G. Han, G. Tu, Diffusion-weighted magnetic resonance imaging for the detection of metastatic lymph nodes in patients with lung cancer: A meta-analysis, Mol. Clin. Oncol. 6 (2017) 344–354.

[235] F. Zhang, Z. Zhou, D. Tang, D. Zheng, J. Cheng, L. Lin, J. Xu, X. Zhao, H. Wu, Diffusion-weighted MRI in solitary pulmonary lesions: Associations between apparent diffusion coefficient and multiple histopathological parameters, Sci. Rep. 8 (2018) 11248.

[236] Y.S. Zhang, J. Aleman, S.R. Shin, T. Kilic, D. Kim, S.A.M. Shaegh, S. Massa, R. Riahi, S. Chae, N. Hu, Multisensor-integrated organs-on-chips platform for automated and continual in situ monitoring of organoid behaviors, Proc. Natl. Acad. Sci. 114 (2017) E2293–E2302.

[237] J.M. Sanders, M.L. Monogue, T.Z. Jodlowski, J.B. Cutrell, Pharmacologic treatments for coronavirus disease 2019 (COVID-19): A review, JAMA 323 (18) (2020) 1824–1836.

[238] J.H. Beigel, K.M. Tomashek, L.E. Dodd, A.K. Mehta, B.S. Zingman, A.C. Kalil, et al., Remdesivir for the treatment of Covid-19—preliminary report, N Engl J Med (2020).

[239] J.-E. Kim, J.-Y. Shin, M.-H. Cho, Magnetic nanoparticles: An update of application for drug delivery and possible toxic effects, Arch. Toxicol. 86 (2012) 685–700.

[240] Y.-H. Xu, J.-H. Dong, W.-M. An, X.-Y. Lv, X.-P. Yin, J.-Z. Zhang, L. Dong, X. Ma, H.-J. Zhang, B.-L. Gao, Clinical and computed tomographic imaging features of novel coronavirus pneumonia caused by SARS-CoV-2, J. Infect. 80 (4) (April 2020) 394–400.

[241] T.S. Higgins, A.W. Wu, E.A. Illing, K.J. Sokoloski, B.A. Weaver, B.P. Anthony, N. Hughes, J.Y. Ting, Intranasal Antiviral Drug Delivery and Coronavirus Disease 2019 (COVID-19): A State of the Art Review, Otolaryngology–Head and Neck Surgery (2020), https://doi.org/10.1177/0194599820933170.

[242] S.S. Nigavekar, L.Y. Sung, M. Llanes, A. El-Jawahri, T.S. Lawrence, C.W. Becker, L. Balogh, M.K. Khan, 3 H dendrimer nanoparticle organ/tumor distribution, Pharm. Res. 21 (2004) 476–483.

[243] Q.A. Pankhurst, J. Connolly, S.K. Jones, J. Dobson, Applications of magnetic nanoparticles in biomedicine, J. Phys. D Appl. Phys. 36 (2003) R167.

[244] J. Owen, Q. Pankhurst, E. Stride, Magnetic targeting and ultrasound mediated drug delivery: Benefits, limitations and combination, Int. J. Hyperthermia 28 (2012) 362–373.

[245] A.S. Lübbe, C. Alexiou, C. Bergemann, Clinical applications of magnetic drug targeting, J. Surg. Res. 95 (2001) 200–206.

[246] A.S. Lübbe, C. Bergemann, J. Brock, D.G. McClure, Physiological aspects in magnetic drug-targeting, J. Magnet. Mag. Mater. 194 (1999) 149–155.